High-Temperature Rubbing: An Effective Method to Fabricate Large-Scale Aligned Semiconducting and Conducting Polymer Films for Applications in Organic Electronics

Shubhradip Guchait, Yuhan Zhong, Martin Brinkmann

High temperature rubbing: an effective method to fabricate large-scale aligned semi-conducting and conducting polymer films for applications in organic electronics

Shubhradip Guchait[1], Yuhan Zhong[1,2] and Martin Brinkmann[1] *

(1) Institute Charles Sadron, Université de Strasbourg, CNRS – UPR22, 67034 France.

(2) ICube Research Institute, Université de Strasbourg, CNRS - 23, Rue du Loess, Strasbourg Cedex 2 67037, France

* Corresponding author : martin.brinkmann@ics-cnrs.unistra.fr

Figure For title of content

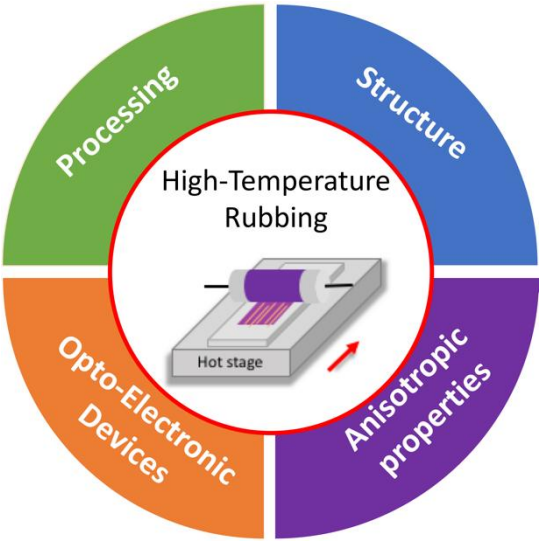

Abstract

Conjugated polymers (CPs) are ubiquitous in plastic electronics in the form of semi-conducting and conducting polymers that are central in devices such as solar cells, field effect transistors and thermoelectric generators. Exploiting the anisotropic properties of such conjugated materials calls for advanced and effective methods of growth and orientation. First, this contribution reviews different alignment methods of conjugated polymers used in plastic electronics. Second, we present the state-of-the-art for the method of high-temperature rubbing that was extensively used to fabricate aligned polymer semiconductors (PSCs) and conducting polymer (CPs) films. Examples are given to illustrate how this versatile method of large scale orientation can be used to design devices with anisotropic opto-electronic properties. Finally, we emphasize the recent progress made in the fabrication of highly ordered and oriented CPs by controlled doping of well crystallized PSCs such as regioregular poly(3-hexylthiophene-2,5-diyl) and Poly[2,5-bis(3-dodecylthiophen-2-yl)thieno[3,2-*b*]thiophene]. The way dopant molecules are introduced into and modify the crystal lattice of these PSCs is presented. The impact of the semi-crystalline structure of the polymers on doping and resulting thermoelectric performances of oriented thin films is discussed.

I. Introduction

Solution-processable Polymer Semi-Conductors (PSCs) are central in plastic electronics as they allow for large scale and low-cost processing for the fabrication of key devices such as Organic Field Effect Transistors, Organic solar Cells and more recently Thermoelectric generators (TEGs).[1-3] Macromolecular engineering has been the route of excellence to fine-tune electronic properties of PSCs and match the requirements in terms of optical and electronic properties to achieve high performances e.g. in organic solar cells for which efficiencies reach record values beyond 15%.[4] Interestingly, the optical and electronic properties of PSCs depend on their structure in the solid state and most of them tend to self-assemble thanks to a segregation between the conjugated polymer backbones and the solubilizing side chains.[5] Self-assembly of PSCs in organic solvents results often, but not exclusively, in the growth of nano-structured objects such as fibrils.[6] More sophisticated growth control of PSCs can generate an even larger palette of morphologies including single crystals, spherulites, nanoribbons or periodic semi-crystalline morphologies e.g. shish-kebab nanostructured fibers.[7-11] Notably, the resulting charge transport properties are impacted by the structural organization of PSCs. Considering the case of regioregular poly(3-hexylthiophene), the crystalline organization is characterized by typical stacking distances, namely the π -stacking of the backbones and the lamellar period between successive π-stacks separated by layers of alkyl side chains (Figure 1). On a larger length scale, PSCs show a structural modulation associated with the alternation of crystalline (ordered) and highly

disordered (amorphous) domains. The coexistence of amorphous and crystalline domains in PSCs relates to their semi-crystallinity that is illustrated for the case of P3HT in Figure 1.a-c.[10]

All these structural features of PSCs have an impact on charge transport in thin films. By essence, charge transport is highly anisotropic in PSCs such as P3HT. Theoretical calculations by Lan et al. suggest that within crystalline domains, with the optimized relative orientation of polymer backbones, the inter-chain charge transport is 2 to 3 order of magnitude slower than the intrachain transport (see Figure 1.d).[12] However, over mesoscopic distances, when charges must travel between crystals, the amorphous regions separating the crystalline domains may interrupt and limit the charge transport along the backbone direction (Figure 1.e). Lan et al. calculated the mobility over several crystalline/amorphous domains taking the amorphous barriers into account and predict a correlation between the charge carrier mobility and the number of crossing points and bridging polymer chains (tie-molecules) inside the disordered region and between the crystalline domains, respectively.

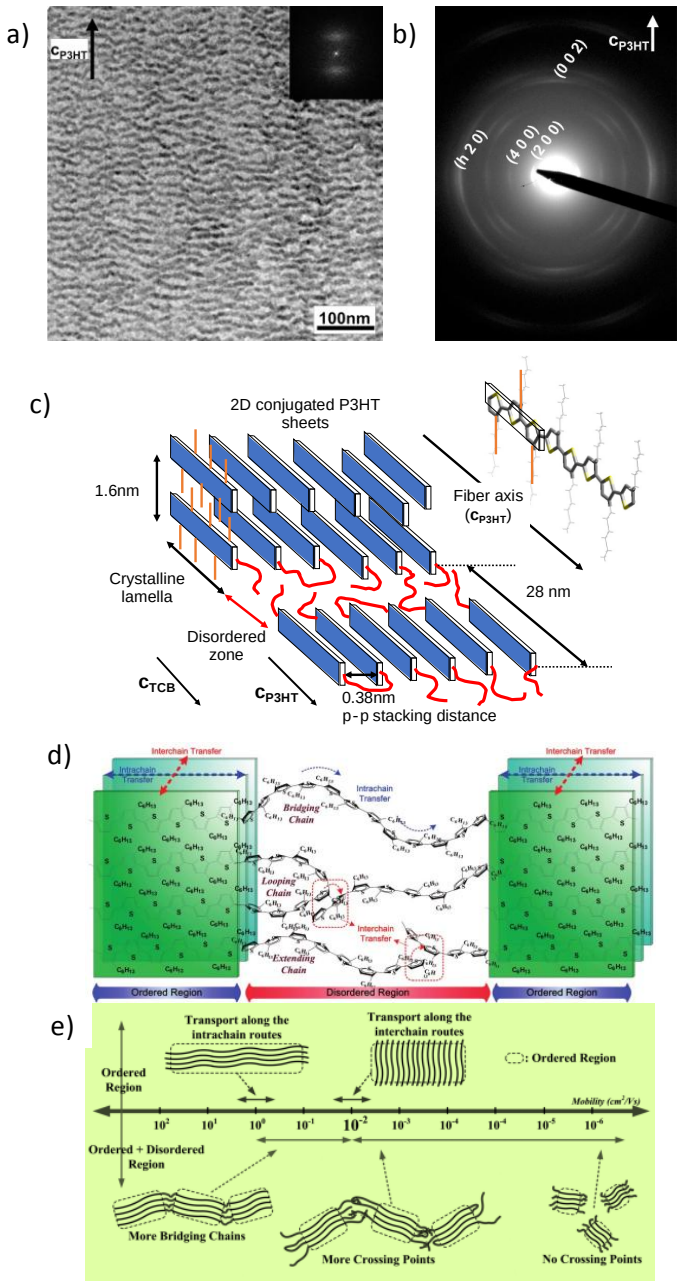

Figure 1*. a) Bright Field TEM image and b) electron diffraction pattern of an oriented RR P3HT thin films aligned by epitaxy on 1,3,5-trichlorobenzene by directional epitaxial crystallization. Note the alternation of dark and bright lamellae in a) that results from the lamellar periodic structure of semi-crystalline P3HT. c) Schematic illustration of the semi-crystalline lamellar structure of RR P3HT showing the different levels of organizations and the associated length scales. d) Schematic illustration of the interface between two crystalline regions through an amorphous zone in RR P3HT. Within the ordered regions (green) the*

inter- and intrachain charge transport paths are indicated. The amorphous zone contains different chain defects such as tie-chains, folds and fully extended chains. e) Illustration of the characteristic length scales for charge transport and the orders of magnitudes of charge mobilities. Figure reproduced with permission from references 10 and 12.

The complex semi-crystalline organization and morphology of PSCs can be exploited to some extent to optimize their transport properties. In particular, PSCs have the ability to be aligned by numerous methods. To cite but a few: shearing, stretching, rubbing, epitaxy and solution-based methods.[13,14] These alignment strategies offer unique opportunities to handle the PSCs morphology and orientation so as to take advantage of their anisotropic optical and electronic properties. Ultimately, aligned PSC films can be used as active layers in the design of electronic devices with anisotropic properties e.g. anisotropic OPV cells, OFETs and polarized photodetectors.

This review is organized in three main parts. First, we present a short and non-exhaustive review of existing alignment methods for semi-conducting polymer films, emphasizing the advantages and disadvantages of the different orientation strategies (see Figure 2 and Table 1). For a more detailed review, we invite the reader to consult the excellent and rather exhaustive work by Pandey et al.[15] Second, we focus on the achievements in the field of thin film alignment using the high temperature rubbing (HTR) method. This method is described in details and the important parameters controlling alignment and structure are reviewed with particular emphasis on the correlation between optimal rubbing temperature (T_R) and molecular weight of the PSCs. Some representative results in organic photovoltaics (OPV), field effect transistors (OFETs) that involve HTR to fabricate aligned active layers are presented. Third, we report recent progress in the fabrication of oriented conducting

polymer thin films by doping of aligned PSC films. We review the strategies that were developed to produce ever more conducting polymer films by a precise tuning of the thin film doping. In this perspective, a short introduction to doping methods of PSCs is given. We present the state-of-the-art in the understanding of the doping of polymer semiconductors and how it is influenced by the semi-crystalline morphology of the PSCs. Finally, we show how the precision in the fabrication of doped aligned PSCs translates in enhanced thermoelectric performances of doped aligned PSCs.

A. Orientation of polymer semi- conductors (PSCs).

Alignment methods can be applied either to the pure (dry) PSCs films in their solid state or in presence of a solvent.[15] The physical processes at play are inherently different. Alignment methods of solid thin films rest on the application of shear stress that can change the polymer chain conformation in the films from coiled to extended chains. Such methods depend essentially on the intrinsic thermomechanical properties of the PSC. In strong contrast, alignment of PSC solutions involves often the lyotropic mesophase of the PSC solution that can be aligned by drawing the solution on a surface. Controlling the evaporation of the solvent helps quench molecular chain orientation upon film formation. In that case, alignment requires a subtle tuning of the evaporation conditions i.e. control over general parameters such as blading speed, temperature, solvent chemical nature, polymer concentration and molecular weight that control the viscosity of the PSC solution. There are multiple variants of the blade coating approach that are rather similar in the involved phenomenon e.g. dip coating, brush coating, or alignment of a swollen PSC film in presence of a magnetic field. A last category of alignment methods makes use of directional molecular

interactions at an interface between a substrate and the PSC, i.e. epitaxy.[13] Epitaxy can involve a solid substrate or, as in directional epitaxial crystallization, a crystallizable solvent such as 1,3,5-trichlorobenzene or naphthalene. In the following, we review briefly these three families of alignment methods. We categorize the existing alignment methods into three families based on their main processing principle: i) PSC solution-based orientation (blade coating, melt-draw method, Dip coating, Brush coating, alignment of a solution under magnetic field), ii) shear-based solid-state orientation methods (strain-alignment, melt-draw alignment, friction transfer) and iii) epitaxial orientation. Finally, we elaborate more extensively on the method of high-temperature rubbing.

1. Solution-based orientation.

Solution-based orientation methods make use of polymer solutions to achieve alignment in thin films after drying of the solvent. There exist multiple solution coating methods that impart orientation to the polymer films e.g. blade-coating, dip-coating and brush-coating. All these methods make use of the subtle interplay between interactions taking place at the different involved interfaces: liquid/substrate; liquid/air and liquid/solid film. Let us review these alignment methods.

1. a. Orientation by blade coating of PSCs.

Blade-coating is a simple effective solution-based alignment method that helps for rapid fabrication of oriented polymer thin films. The efficacy of this alignment technique depends mainly on the coating speed, the distance between blade and surface and the surface temperature during blading. As such, this alignment method is a meniscus-determined process that rests on the physico-chemical phenomena occurring at the interfaces between the solution, the solid film, the air and the solid substrate.[16] The surface energy of the

substrate and the surface tension of the polymer solution play important roles on the resulting thin-film microstructures.[17-19] Zhang and coworkers have shown that blade coating involves two distinct regimes depending on the blading speed: i) the Landau-Levich regime (a draining regime) and ii) the capillary (or evaporative) regime. The transition between these regimes has been investigated intensively for polymers such as PCDTPT (poly[4-(4,4-dihexadecyl-4H-cyclopenta[1,2-b:5,4-b']dithiophen-2-yl)-alt-[1,2,5]thiadiazolo[3,4-c]pyridine]) and CDTBTZ (poly-[2,6-(4,4-bis-alkyl-4H-cyclopenta[2,1-b;3,4-]-dithiophene)-alt-4,7-(2,1,3-benzothiadiazole)]). To be in the evaporation regime, the coating speed must be at a moderate rate of 0.4 mm s^{-1} (for a solvent made of 1:3 oDCB : chloroform by volume for coating solvent at 30°C). In the evaporative regime, the polymer chain director is oriented perpendicular to the blading direction.[19]

This technique was further improved using a home-made blade-coating system as shown in Figure 2, by playing for instance with the angle between the blade and the substrate. Using in-situ Grazing Incidence Wide Angle X-ray Scattering (GIWAXS), the authors demonstrated that aligned seed crystals formed in the early stage in the Landau-Levich regime serve as a templates for the bulk alignment during the subsequent drying process.[20,21] The Ludwigs group used the blade coating method to align the n-type polymer P(NDI2OD-T2), which has a strong tendency to aggregate in solution. Remarkably large-area orientation of polymer films with a dichroic ratio of 18 and high transport anisotropy were demonstrated.[22]

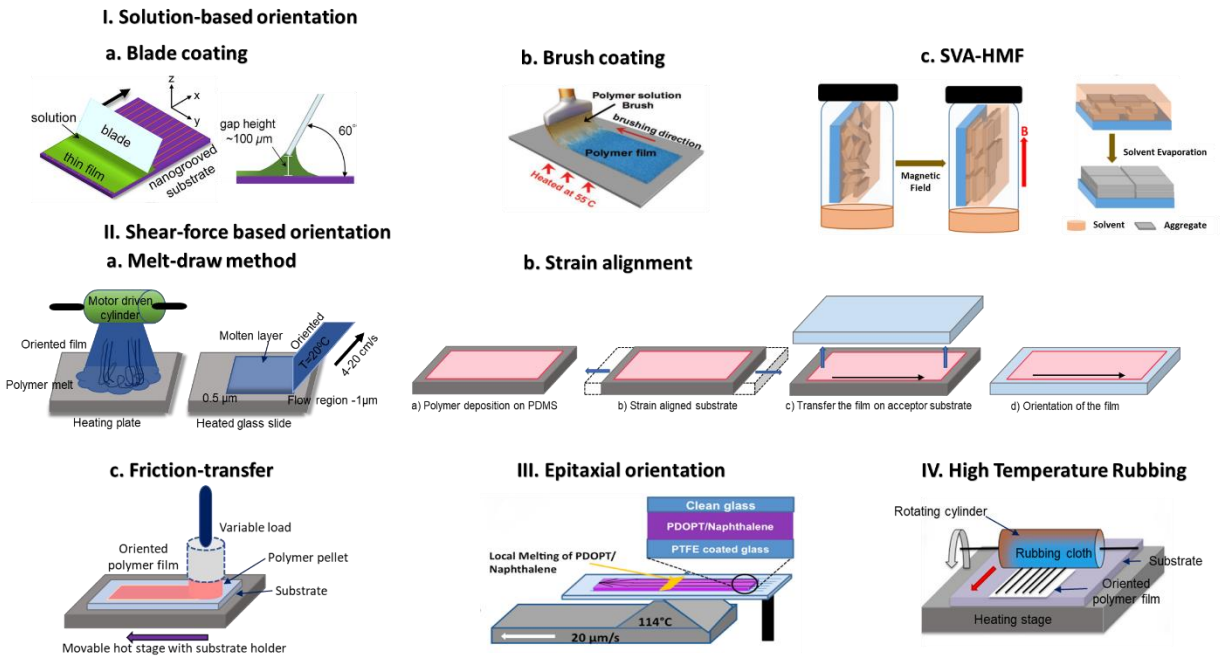

Figure 2: *Schematic illustration of some representative PSC alignment methods for different types of organic electronics applications. I. Solution-based orientation. a) Blade coating, the blade angle is maintained at 60° and a gap height is set to approximately 100 μm. The blade is translated parallel to the substrate at a constant speed that depends on the temperature and solvent. b) Brush coating, schematic diagram of the brush-coating process. c) Solvent vapor annealing under high magnetic field (SVA-HMF), sketch representation of this process for the alignment of P(NDI2OD-T2) polymer thin films. II. Shear-force based orientation. a) Melt-draw method, instrumental setup to prepare highly oriented ultrathin polymer films. b) Strain alignment, this method involves four steps, i) deposition of the polymer film and transfer to PDMS substrate of 2 mm thickness, ii) applying the strain to stretch the PDMS substrate and align the PSC film, iii) transfer the strained PSC film on the target substrate by pulling off the PDMS slab. c) illustration of the alignment method by friction transfer. III. Epitaxial orientation, schematic illustration of the directional epitaxial crystallization method of PDOPT using naphthalene as a crystallizable solvent and IV. High Temperature Rubbing,*

schematic illustration of high temperature rubbing apparatus consisting of a rotating cylinder and a heating sample holder.

I. b. Brush coating of PSCs.

In this alignment technique, a brush is usually immersed into the polymer solution and spread over the substrates to form aligned thin films in the drawing direction. The degree of alignment is significantly higher in brush coated films than in drop casting.[23] The driving force for the alignment results from a subtle interplay between two effective shear stress forces acting at two liquid-solid solution-substrate and solution-brush interfaces. Guo et al. used this technique to induce orientation in semiconducting and conducting polymers such as P3HT, P(NDI2OD-T2) and PEDOT: PSS.[24] Recently Lin et al modified this technique by replacing the conventional brush with a Chinese brush (C-brush) that is made from multiscale structured hairs of animals (FE-hairs) (see Figure 2).[25,26] They reported that the control of parameters like brushing speed, substrate temperature and solution concentration can help to tune the contact at the liquid/air/solid interfaces to prepare highly oriented films by self-assembly of polymer backbones in the translation direction. With this process the same group has reported an optical dichroic ratio of 2.89 for C-brush-coated films of poly [2,5-(2- octyldodecyl)-3,6-diketopyrrolopyrrole-alt-5,5-(2,5-di(thien-2-y) thieno[3,2-b] thiophene)] (DPPDTT). The best hole mobility approached 6.2 $cm^2 V^{-1} s^{-1}$ in the chain direction which is six times higher than that of spin-coated DPPDTT.[25,26]

I.c. Solvent Vapor Annealing under High Magnetic Field (SVA-HMF).

As demonstrated by Zhang and coworkers , the application of a high magnetic field (HMF) (~8-9 Tesla) for several hours is a versatile non-contact method to enforce molecular alignment and grow large areas of oriented organic materials.[27] The driving force for

orientation rests on the anisotropy in the diamagnetic susceptibility of organic molecules and minimization of the molecular free energy in the magnetic field. Zhang et al. investigated the use of HMF to orient films of the donor-acceptor copolymer poly{[(N,N'-bis (2-octyldodecyl) -1,4,5,8-naphthalene dicarboximide)-2,6-diyl]-alt-5,5'-(2,2'-bithiophene)} [P(NDI2OD-T2)], by drop-casting the film in the presence of HMF. [27] However, the alignment is very much dependent on the drying process because of de-wetting of the polymer film from the substrate (see Figure 2). For this reason, the group combined HMF alignment with a controlled solvent vapor annealing (SVA) of the thin films to overcome the difficulties linked with the drying process. SVA employs saturated solvent vapors to swell or partially dissolve organic materials, which conveys the molecules with a higher mobility to reorganize and enhance molecular ordering and film crystallinity. It has been demonstrated that SVA-HMF is an effective method to align a large set of organic systems including, liquid crystals, block co-polymers and donor-acceptor copolymers. Apart from controlling in-plane orientation, Pan et al. reported important out-of-plane molecular orientation of P(NDI2OD-T2) films under HMF (9 Tesla) for 8h.[28]

II. Alignment based on shear forces.

II.a. Melt-draw alignment.

The melt-draw technique was introduced by Petermann and Gohil in 1979 for polyolefins such as polyethylene (PE).[29] The experimental setup consists of a heating glass plate and a cylinder driven by a motor. The polymer solution is spread uniformly on the flat glass substrate on a heating plate (see Figure 2). The temperature is set generally above the highest crystallization temperature of the supercooled polymer melt. After evaporation of

the solvent, a motor-driven cylinder with a speed of approximately 4 ~ 20 cm s^{-1} is used to pull a thin film at constant speed. The thickness of the melt-drawn films is usually in the 30-60 nm range. To prepare highly oriented polyethylene films, the temperature is set to a temperature above 120 °C. Parallel-arranged edge-on lamellae are formed in the melt-drawn films with the lamellae aligned in the direction perpendicular to the drawing direction. Various parameters such as structure, morphology as well as crystal structure of polymorphic polymers such as syndiotactic polypropylene can be controlled by the take-up speed and sample temperature during drawing. With increasing take-up speed and decreasing temperature, orientation of the films improves and shish kebab structures become prominent for PE.[30,17] Bio-sourced polymers such as poly(lactic acid) were also recently aligned by this method.[31] So far, no attempts have been made to adapt this method to conjugated polymers such as P3HT.

II. b. Strain-alignment of PSC films.

Alignment of most polymers can be achieved by application of strain whereby the chain conformation is modified and alignment of polymer chains usually occurs in the direction of applied strain. This approach was applied to PSC thin films generate anisotropic charge transport properties in aligned PSC films. O' Connor et al investigated the method of strain-alignment for regioregular P3HT.[32] For this polymer, an optical dichroic ratio of 4.8 and a charge-mobility anisotropy of 9 in OFETs were achieved. From a technical point of view, the polymer film is first deposited on a substrate made of octyltrichlorosilane modified oxidized silicon (OTS–Si) by spin-coating. Second, the P3HT film is transferred from the OTS-Si substrate on a polydimethylsiloxane (PDMS) slab (2 mm thickness) by lamination. The PDMS slab supporting the P3HT film can be stretched by applying strain. Increasing levels of strain

result in improved alignment levels. Finally, once strained, the P3HT film is transferred from the P3HT/PDMS slab to a target substrate (glass or a silicon wafer with 230nm thermal oxide layer, see Figure 2). During the strain process the polymer film undergoes plastic deformation, P3HT nanocrystals align with the chain direction parallel to the direction of the applied strain. One disadvantage of strain-alignment methods relates to potential mechanical fracture and cracking of the films. This is why macromolecular engineering was used to produce PSCs that are more resilient to such mechanical constraints. One promising strategy consists in the engineering of the PSC side chains using for instance siloxane side chains to impart better thermomechanical properties and obtain PSCs that are more resilient to mechanical strain.[33]

II.c. Friction-transfer alignment.

Friction-transfer was originally used by Wittmann and Smith to prepare ultra-oriented and highly crystalline thin films of poly(tetrafluoroethylene) (PTFE).[34] Such oriented PTFE films proved very effective as alignment layers for epitaxial crystallization of small molecules and polymers.[35-39] The group of Yase extended this friction transfer method to conjugated polymers such as poly(alkylthiophene)s (P3ATs). In practice, a polymer pellet is pressed on a hot substrate and dragged across it at a constant speed whereby a thin oriented film is deposited on a substrate. Accordingly, a major advantage of this alignment method is that no solvent is necessary and alignment can be performed for poorly soluble polymers. Orientation can be remarkably high with DR up to 100 for poly(3-dodecylthiophene). Similarly to high-T rubbing, friction transfer imparts a dominant face-on orientation of aligned P3AT crystals in the thin films. The resulting charge mobility shows very high charge

mobility anisotropy ratios with $\mu_{//}/\mu_{\perp}$=8 ($\mu_{//}$ and $\mu_{\perp}$ are the charge mobilities measured in the directions parallel and perpendicular to the rubbing direction). Beside poly(3-alkylthiophene)s, friction transfer was successfully applied to numerous other PSCS including poly(9,9-di(n-octyl)-fluorene-2,7-diyl) (PFO), poly(dimethylsilylene), poly(p-phenylene)and poly(2,5-dioctyloxy-1,4-phenylenevinylene). Most interestingly, the friction transfer of PFO was successfully used to prepare polarized light emitting diodes.[38]

III. Epitaxial orientation of PSCs.

Epitaxy is basically a directional growth of a crystalline or semi-crystalline material which operates via a crystalline substrate that stimulates/directs the over-layer's growth.[40] Unlike inorganic epitaxy, the epitaxy of organic materials as well as polymers is controlled by a subtle balance of weak noncovalent interactions at the interface between substrate and overlayer. From a structural and morphological point of view, polymer epitaxy was thoroughly investigated by Lotz and Wittmann using transmission electron microscopy.[41,42] Oriented growth of crystalline lamellae of polyethylene was demonstrated by epitaxy on aromatic crystal substrates such as anthracene or *p*-terphenyl. These molecules can form large single crystal surfaces that are ideal for epitaxial crystallization of the polymers with moderate melting temperature such as PE. Aromatic salts such as potassium-4-bromobenzoate (K-BrBz) or potassium acid phthalate (KAP) are ideal substrates for epitaxy of polymers with melting temperatures up to 300°C.[43] In all cases, this method implies first to grow sufficiently large single crystal substrate surfaces of a few hundreds μm^2 up to several mm^2. A polymer film is deposited a top the single crystals prior to melt-crystallization of the polymer film to induce epitaxy. The substrate material is removed e.g. by rinsing with an appropriate solvent or by evaporation under primary vacuum.[44-46] Thierry and coworkers

applied this approach to orient diacetylenes over large surfaces.[46] Later on, Brinkmann et al. applied epitaxial growth to design specific orientations and patterns of crystalline P3HT crystals on potassium bromo-benzoate (K-BrBz).[45] The method of directional epitaxial crystallization was implemented by the Salleo group to probe the anisotropy of charge mobilites in oriented P3HT films.[47] Charge mobility larger than 10^{-2} $cm^2/V{\cdot}s$ were observed in the chain direction and the anisotropy of charge mobilities $\mu_{//}/\mu_{\perp}$ was larger than 10.

Brinkmann et al have used directional epitaxial crystallization which is a variant of epitaxy to align many different polymers such as poly(3-hexylthiophene (P3HT), poly(9,9-di(n-octyl)-fluorene-2,7-diyl) (PFO) and poly(3-(2,5-dioctylphenyl)-thiophene) (PDOPT).[48-54] They used a crystallizable aromatic solvents such as 1,3,5-trichlorobenzene (TCB) or naphthalene to act as i) the solvent for the polymer when the crystallizable solvent (CS) is molten and ii) as a substrate for epitaxy once crystallized. Large-scale orientation of the PSC implies a well-controlled growth of the CS over large areas. This is achieved by using the instrumental setup shown in Figure 2.III. The polymer is first dissolved in the CS (for instance naphthalene for PDOPT) and the resulting PSC/CS solution spreads by capillarity between two glass substrates. After solidification of the PSC/CS solution, a zone melting technique is used at a preset temperature at the pyramidal tip in contact with the PSC film.[51,53] A steady and slow crystallization of the CS is enforced (typically at 20 μm/s as depicted in Figure 2). After this orientation step, vacuum is applied in order to evaporate the CS, leaving large areas (several mm^2) of highly oriented polymer film on a given substrate (glass, Si wafer, etc…). In the case of poly(3-(2,5-dioctylphenyl)thiophene) (PDOPT), directional epitaxial crystallization on naphthalene resulted in alignments with dichroic ratios of the absorption and photoluminescence in the 8-10 range.[51] Single-crystal-like electron diffraction patterns helped to refine the crystal structure of PDOPT (Figure 3).

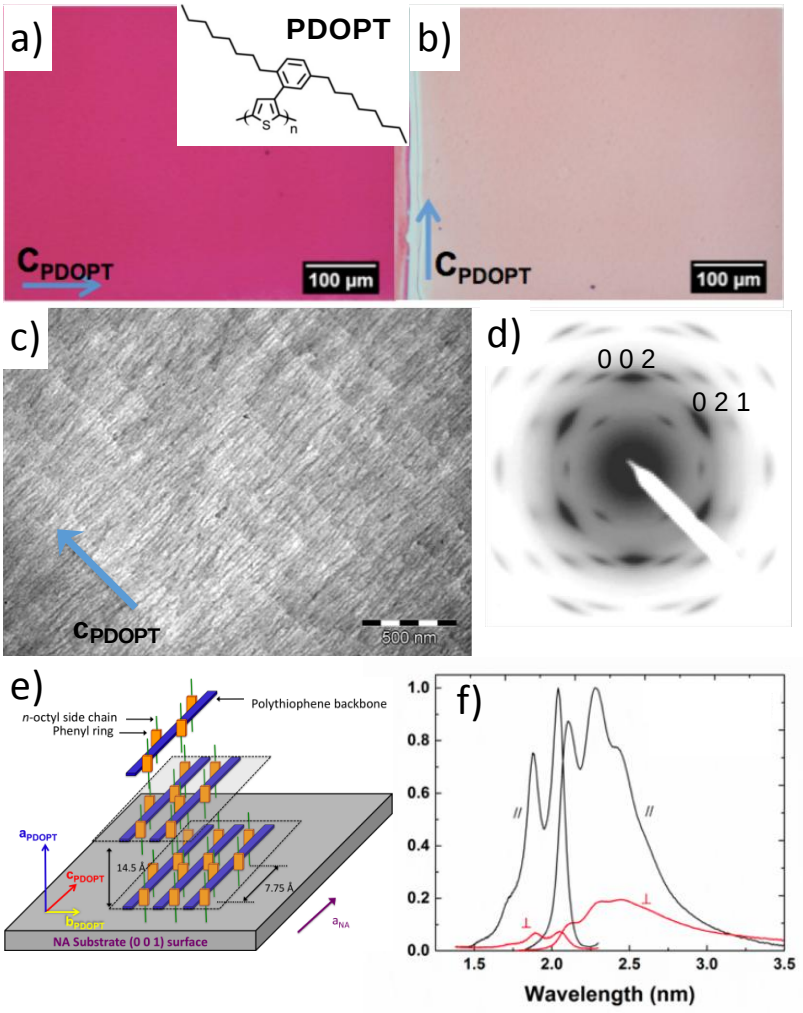

Figure 3. *POM images of oriented PDOPT films aligned by epitaxy on naphthalene for light polarized in the chain direction (a) and perpendicular to it (b). The chemical structure of PDOPT is shown as an insert in a). The direction of PDOPT chains is highlighted in blue and the light polarization by a black double arrow. C) and d) TEM bright field showing the oriented PDOPT lamellae and electron diffraction pattern of an oriented PDOPT film. The chain direction in the BF image is indicated by a blue arrow. E) Illustration of the dominant contact plane of PDOPT crystals in oriented thin films and relative orientation to the naphthalene substrate crystal. F) Polarized absorption and luminescence spectra of PDOPT films aligned by epitaxy on naphthalene substrate. For the luminescence, the light excitation was at λ=540 nm. Reproduced from reference 51.*

Epitaxy can also be realized on polymeric substrates such as oriented poly(tetrafluoroethylene) (PTFE) prepared by friction transfer.[55] Polyfluorenes such as poly(9,9-bis(n-octyl)fluorene-2,7-diyl) (PFO) and poly(9,9-bis(2-ethylhexyl)fluorene-2,7-diyl) (PF2/6) were readily oriented by crystallization from the melt on substrates of oriented PTFE. The crystalline lamellae were observed to grow essentially perpendicular to the PTFE chain direction and the epitaxial conditions were determined as $[0\ 0\ 1]_{PF}//[0\ 0\ 1]_{PTFE}$ and $(0\ 1\ 0)_{PF}//(1\ 0\ 0)_{PTFE}$. Evidence for extended-chain crystallization of PF2/6 was provided by the scaling between lamellar periodicity and average molecular weight of the polymer.

IV. High Temperature Rubbing.

Mechanical rubbing is an established orientation technique for polymer thin films which involves the use of surface shearing forces at the interface between a rotating cylinder and a polymer film.[56,57] One can align different polymers over large areas (several cm^2) with the help of shearing forces in the rubbing direction. The mechanical rubbing method has been extensively used in the liquid crystal display industry to prepare oriented polyimide layers. Mechanical rubbing at room temperature (RT) was further applied to PSCs such as P3HT by Heil et al.[58] Significant mobility enhancement was reported by Heil and coworkers in OFETs prepared by rubbing regioregular (RR) P3HT at ambient temperature.[58] Polymer orientation with mechanical rubbing was also studied as a function of molecular weight of P3HT by Hartmann et al. [53] It was reported that P3HT with low molecular weight can be readily oriented by rubbing at RT whereas for $M_w \geq 50$ kDa, chain entanglements and tie chains linking crystalline domains hinder reorientation of domains at room temperature. Later on,

the Brinkmann group systematically studied the impact of two parameters, temperature and molecular weight on the alignment level in rubbed P3HT and PBTTT films.[53, 59-62] To this end, they have modified the mechanical rubbing technique by introducing a heating stage supporting the polymer film during rubbing (see Figure 2). A rotating cylinder covered with a microfiber cloth, is translated over the polymer thin film on a substrate maintained at a certain temperature. Figure 4 presents an overview of some representative PSCs that were aligned by HTR and shows the polarized UV-vis spectra together with their electron diffraction patterns. The rubbing temperature (T_R) needs to be optimized for each polymer taking into account their macromolecular parameters. Using rubbing temperatures near to the melting helps reach very high crystallinity in P3HT in addition to alignment and the temperature modifies the lamellar periodicity of the polymer (see Figure 5). As a general mechanism, shear forces generate bundles of highly oriented polymer chains that can act as oriented seeds for the crystallization of the entire polymer film. It helps to form anisotropic PSC films with enhanced charge transport in the alignment direction.[62]

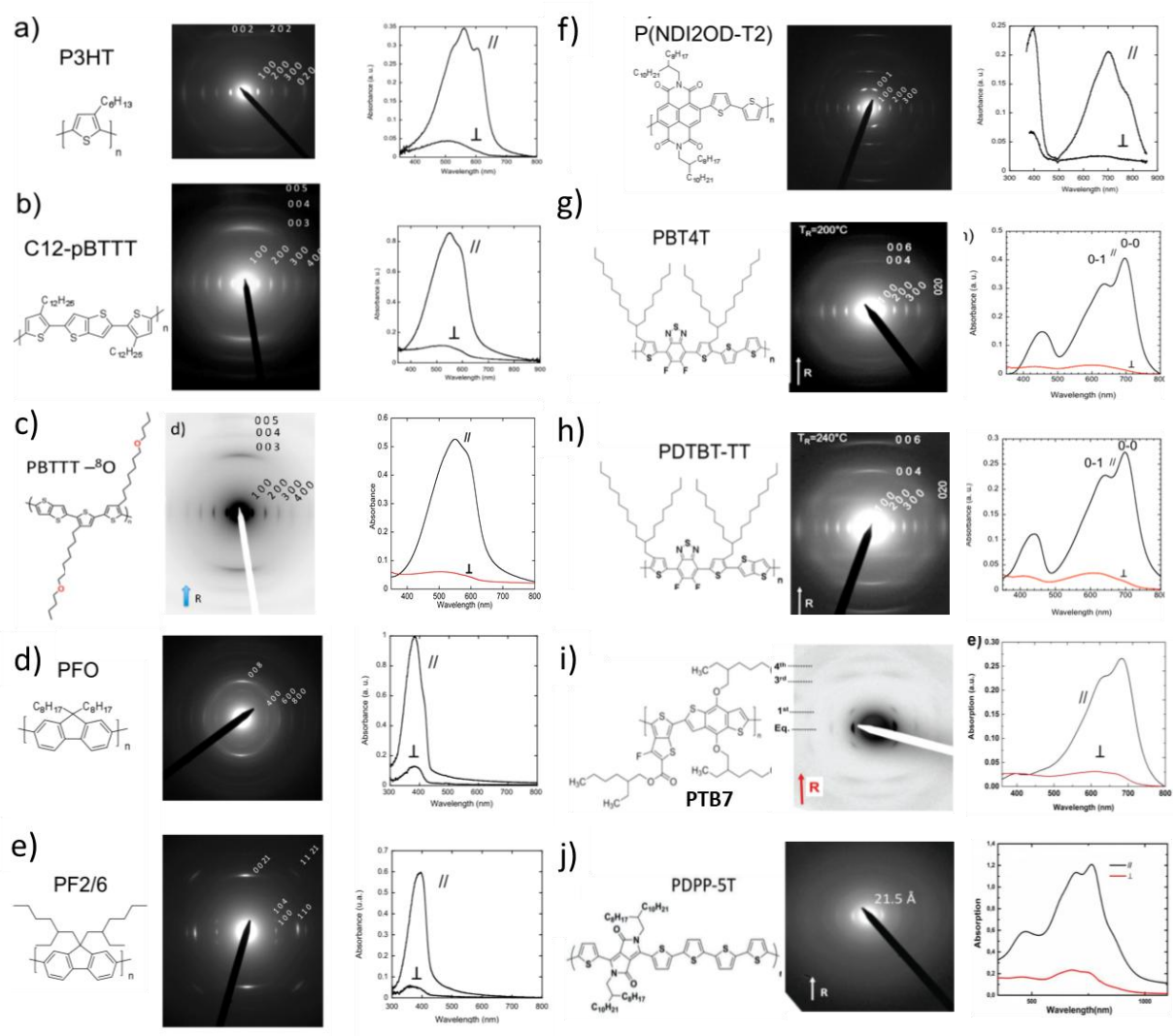

Figure 4: *Electron diffraction patterns and polarized UV–vis absorption spectra (for parallel (∥) and perpendicular (⊥) orientations of the incident light with respect to the rubbing direction) of highly oriented thin films of semiconducting π-conjugated polymers prepared by high-temperature rubbing. The chemical structures of the polymers are shown on the left.* T_R*= 180 °C for P3HT (*M_w *= 53 kDa),* T_R*=125°C for* C_{12}*-PBTTT films (*M_w *= 45 kDa),*T_R*=170°C for PBTTT-*^{8}*O (*M_n*=30.2 kDa),* T_R*=125°C for PFO films (*M_w *= 56 kDa) that were subsequently annealed at 210 °C. PF2/6 films (*M_w*= 147 kDa) were rubbed at 190 °C and annealed at 200°C, P(NDI2OD-T2) films (*M_w*= 19.3 kDa) were rubbed at 80 °C and annealed at 280 °C, TR=200°C for PBT4T (*M_w*= 80kDa),* T_R*=220°C for PDTBTT-TT (*M_w*= 13 kDa). PTB7 (*M_w *= 87 kDa) were rubbed at* T_R*=200 °C and subsequently annealed at 260 °C for 1h.* T_R*=125°C for*

PDPP-5T (M_w = 50.0 kDa). Indexing of the electron diffraction patterns was performed using the structures published in the literature (52, 58-65). Reproduced and adapted from reference 62.

High-T rubbing (HTR) was applied with success to various classes of π-conjugated polymers including semi-flexible or hairy-rod-like polymers such as PFO or PBTTT.[62] Other n-type polymers such as P(NDI2OD-T2) or polymers used in OPV (PCPDTBT and PTB7) could also be aligned by high-T rubbing.[63-66] From a structural perspective, most studies showed that rubbing induces a change of the crystal contact plane from edge-on in pristine unrubbed films to mainly face-on crystals after alignment. Figure 4 collects the typical electron diffraction patterns and the polarized UV-vis spectra of ten PSCs, underlying the high potential and versatility of this orientation method for PSCs.

Among the most studied systems using high-T rubbing is regioregular P3HT (RR P3HT) that can be considered as a model system for this alignment method. Hamidi-Sakr et al. investigated the impact of molecular weight and temperature on the structure and morphology of rubbed RR P3HT.[61] With the help of polarized UV-Vis spectra, Hamidi-Sakr et al. evidenced the dependence of the orientation parameter of polymer chains on the rubbing temperature. For T_R= 170°C the maximum orientation factor is achieved in RR P3HT (OP=0.83) and a clear vibronic structure is seen in the UV-vis absorption spectrum (Figure 5.a-b). In strong contrast; when the light is polarized perpendicular to the rubbing, an unstructured and 550 nm-centered absorption is observed. This is the fingerprint of the amorphous interlamellar zones of RR P3HT. With increasing T_R (170°C to 217°C) the intensity of the 0–0 component in the vibronic structure of the UV-Vis spectrum increases indicating enhanced chain planarization as a consequence of increasing crystal stem lengths. This

enhanced planarity with increasing rubbing temperature is also visualized using TEM electron diffraction and High Resolution TEM.[61]

High-T rubbing induces crystals to change their contact plane from edge-on to face-on at moderate T_R. When the rubbing temperature approaches the melting, however, the films tend to adopt a so-called fiber symmetry i.e. the chain direction is parallel to the rubbing but multiple contact-planes are possible (see Figure 5).[61,44] With increasing temperature from 98°C to 144°C, electron diffraction shows a set of equatorial h 0 0 reflections instead of the 0 2 0 Scherrer ring which indicates a significant transformation from nonaligned edge-on to face-on P3HT domains. For T_R < 144 °C, the oriented RR P3HT forms a smectic-like phase. The smectic-like phase is made of π-stacks of P3HT chains separated by disordered layers of 3-hexyl side chains and with statistical disorder in the chain direction indicating no registry in the stacking of thiophene monomers within individual π-stacks. (52) For $T_R \geq 144$ °C, P3HT films form a semi-crystalline structure and for T_R=217 °C the electron diffraction patterns show numerous mixed index reflections indicating high crystalline order.[61]

Hamidi-Sakr et al. characterized the semi-crystalline lamellar structure of P3HT made of alternating crystalline and amorphous zones by Transmission Electron Microscopy.[61] The lamellar periodicity is controlled by the rubbing temperature.

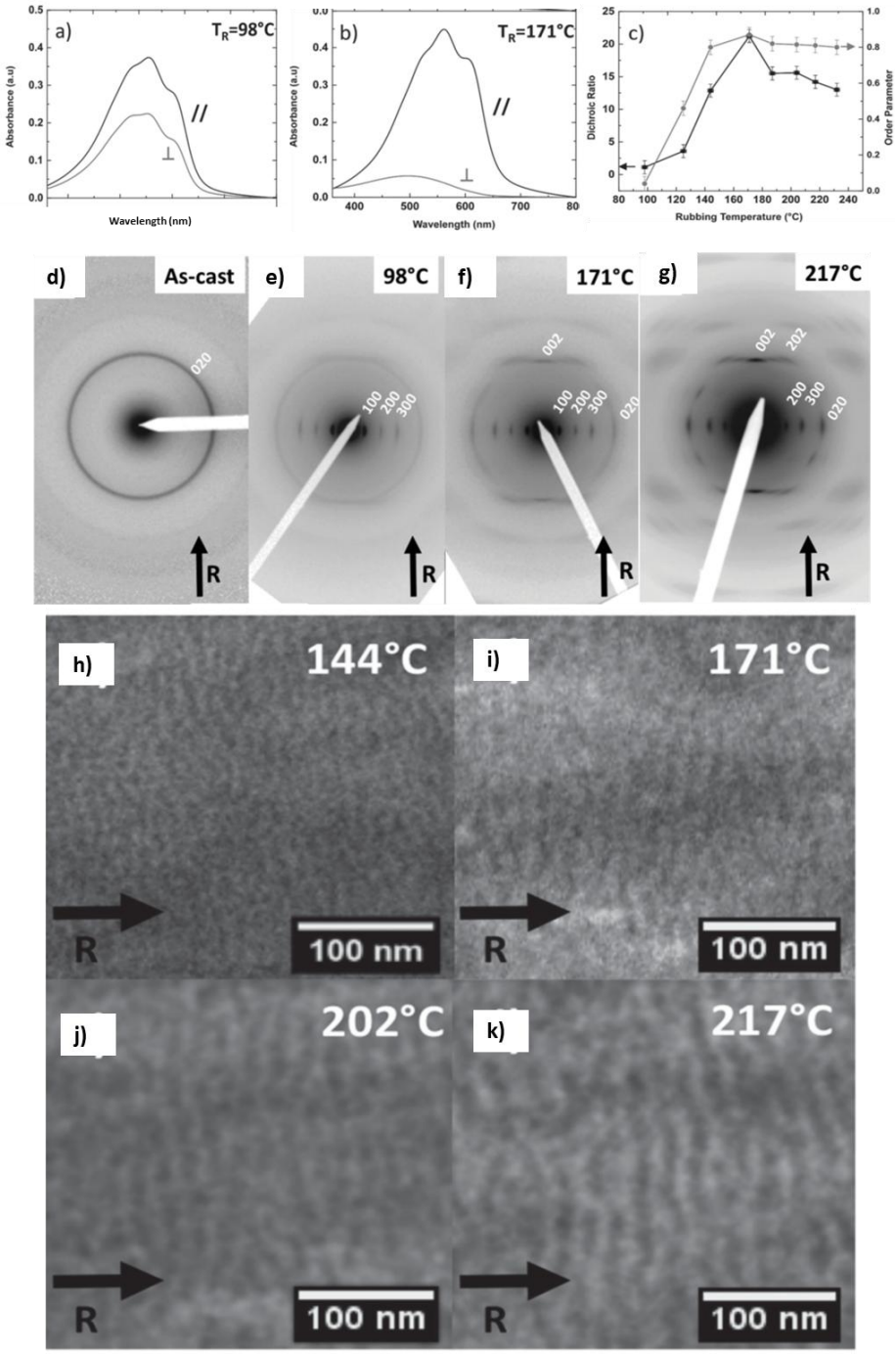

Figure 5: *Polarized UV–vis spectra of oriented P3HT films (M_w = 50 kDa) recorded with rubbed film at a) rubbing temperature T_R = 98 °C and b) 171 °C. c) Evolution of the dichroic ratio (DR) at 610 nm (full squares) and of the 3D order parameter (full grey circles) defined as (DR− 1)/(DR+2) at different rubbing temperatures. d–g) Evolution of the ED diffraction patterns in rubbed P3HT films as a function of the rubbing temperature T_R. For each ED pattern, the*

direction of rubbing (R) is indicated by an arrow. h)-k) Evolution of TEM bright field images of the lamellar morphologies in rubbed P3HT films as a function of T_R. Adapted and reproduced from reference 61.

A more systematic investigation of the impact of molecular weight on orientation was made by Biniek et al. for RR P3HT as well as C_{12}-PBTTT (see Figure 6).[59,62] The alignment of three different polymer fractions of P3HT was investigated by polarized spectroscopy (low-M_w (7.9 kDa, PDI = 1.1), medium-M_w (M_w = 43 kDa, PDI = 1.8) and a high-M_w (M_w = 53 kDa, PDI = 1.5)). Figure 6.g shows the dichroic ratio of rubbed P3HT films as a function of M_w. Low-M_w P3HT exhibits high orientation when rubbed at ambient temperature, whereas to achieve similar orientation, medium- and high-M_w samples require rubbing at 75 °C and 125 °C, respectively.[59,62]

The importance of the rubbing temperature on the alignment and structure was further investigated in a systematic way for the polymer C_{12}-PBTTT (M_n = 27 kDa) using polarized UV-Vis-NIR spectroscopy and TEM diffraction.[62] Again, T_R and M_w have a very strong impact on the achieved alignment in C_{12}-PBTTT thin films (Figure 6.a). The DR increases gradually from less than 2 (T_R = 23 °C) to 8–10 (T_R = 125 °C). For $T_R \geq$ 125 °C, the polymer layer are delaminated from the substrate because the films are rubbed in their liquid crystalline phase formed around 130 °C.[67-69] This result indicates that the in-plane alignment of C_{12}-PBTTT chains improves substantially with increasing T_R and that alignment of this polymer by HTR must be performed in the crystalline phase with a partial disordering of the alkyl side chains, but not in the mesophase. TEM ED demonstrates mainly face-on orientation of C_{12}-PBTTT domains with marginal presence of edge-on oriented domains (see Figure 6.b-f). To verify the impact of the M_w of C_{12}-PBTTT on alignment by high-T rubbing, three different M_w fractions of C_{12}-PBTTT were aligned (see Figure 6). As seen in Figure 6.h,

high M_w samples need higher T_R to reach equivalent alignment. These experiments on RR P3HT and C_{12}-PBTTT evidence the strong dependence of the alignment by rubbing on the molecular weight of the polymer.[62,65]

More recently, Durand et al. aligned PBTTT-^{8}O polymer (M_n=30.2 kDa) by HTR. This polymer has the same backbone as C_{12}-PBTTT but the *n*-C_7–O–C_4 side chains differ from *n*-C_{12}.[70,65] Interestingly, the use of single-ether side chains made it possible to align PBTTT-^{8}O in a large temperature range (100°C –240°C) without delamination of the LC phase as observed for PBTTT-C_{12}. A very high DR=22 was obtained for T_R=170°C corresponding to a 3D order parameter, S= $(\frac{DR-1}{DR+1})$ = 0.86. DR was observed to progressively increase in the range 80°C ≥T_R≥170°C and subsequently decreases as T_R approaches the melting temperature (T_m = 250°C).

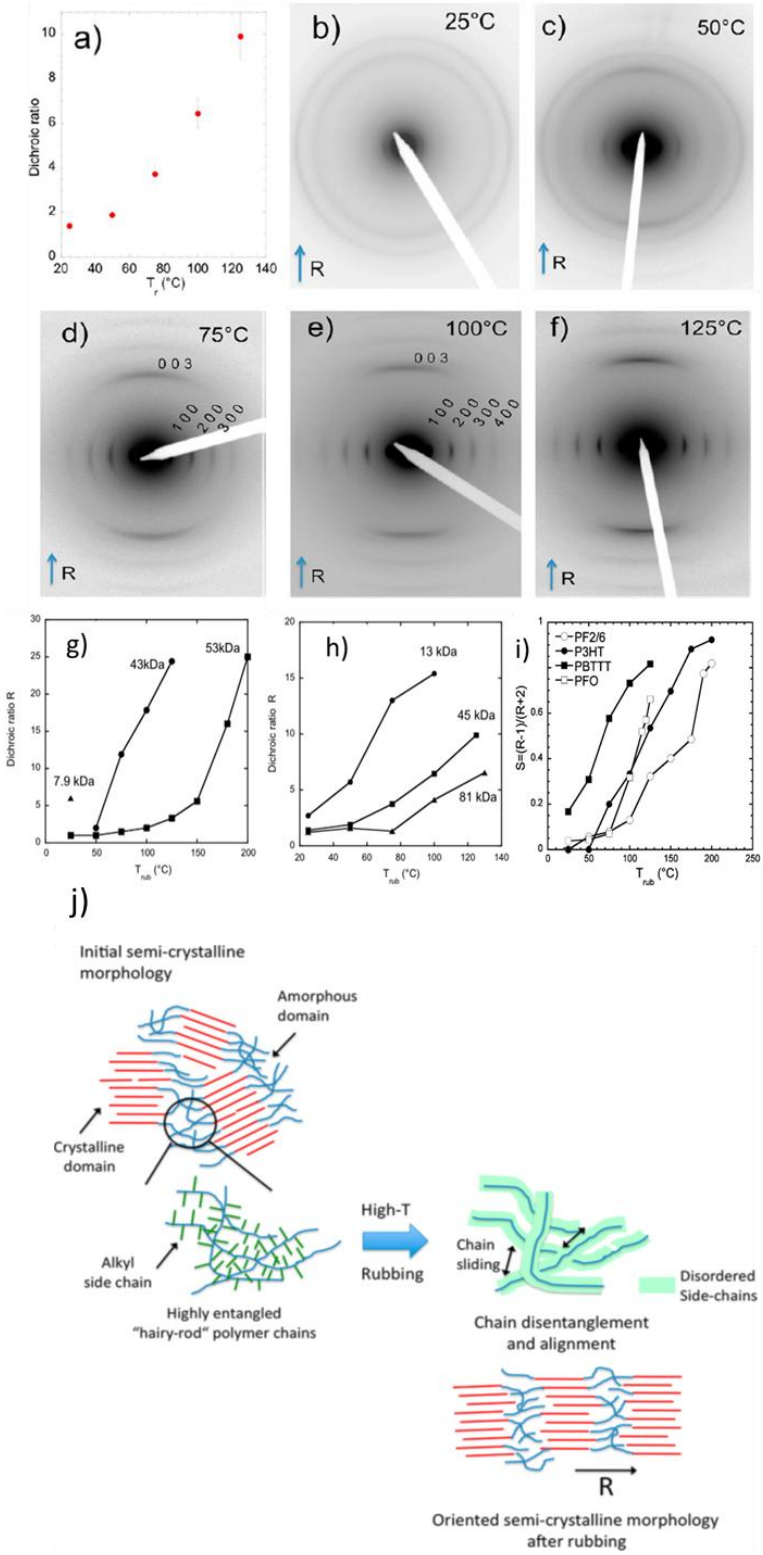

Figure 6: *a) Dependence of the dichroic ratio at 550 nm with the temperature during rubbing T_R of C_{12}-PBTTT thin films. b–f) TEM ED patterns of the C_{12}-PBTTT films rubbed at different temperatures in the range 23–125 °C. The rubbing direction R is indicated by arrow. T_R-*

dependence of the DR at 605 nm for P3HT (g) and C_{12}-PBTTT (h) thin films rubbed as obtained for different molecular weights. As a means of comparison, the DR of a P3HT 7.9 kDa sample rubbed at 25 °C is shown in part g. (i) Evolution of the order parameter S = (R − 1)/(R + 2) calculated from the UV−vis absorption DR (R) for rubbed semiconducting polymer films as a function of T_R. j) Schematic illustration explaining the role of side chain melting on the disentanglement of polymer tie chains that is necessary to completely re-orient polymer domains during the HTR process. Reproduced and adapted from reference 62.

Zeng et al. demonstrated that the population of face-on crystal orientation is dominant for 80°C ≤T_R≤170°C whereas edge-on orientation of the crystalline domains is prevalent for T_R≥200°C. For T_R=170°C, the films consist of a mixture of face-on and edge-on orientations.[65] Overall, these results demonstrate that the efficiency of HTR is also determined by the chemical nature of the side chains that controls the thermomechanical properties of the PSCs.

In addition to polythiophenes, HTR proved very effective to align polymers such as polyfluorenes that show interesting electroluminescence properties.[62] The alignment of two polyfluorenes was studied, namely poly(9,9-di(n-octyl)-fluorene-2,7-diyl) (PFO) with linear n-octyl side chains and poly(9,9-bis(2-ethylhexyl)fluorene-2,7-diyl) (PF2/6) with branched 2-ethylhexyl side chains. Both polymers align by rubbing at T_R≥100 °C. ED analysis indicated that T_R≥100 °C is not sufficient to induce crystallization of the films but additional thermal annealing is necessary to improve orientation. Importantly, the work on polyfluorenes demonstrated that the choice of the solvent used for the preparation of the pristine non-oriented PSC film has a major impact on alignment, polymorphism and crystallinity of the rubbed films. PFO films prepared from chloroform lead to better alignment than films

prepared from chlorobenzene, suggesting that poorly ordered films of polyfluorene polymers align more readily upon rubbing than highly crystalline ones. Notably, post-rubbing annealing helped improve the orientation and crystallinity of the rubbed PFO films. As seen in Figure 6.i, a simple comparison among the different alignment levels for polythiophenes and polyfluorene polymers can be made by plotting the order parameter S as a function of T_R for different polymers. All polymers show a similar trend: S increases consistently with T_R up to a certain point, thanks to the softening of side chains that eases in-plane alignment by rubbing.[62] Brinkmann and coworkers demonstrated that the impact of M_w and temperature are general for most PSCs made of conjugated backbones and soft alkyl side chains. A general alignment mechanism was thus proposed (see Figure 6.j). Rubbing is a means to create aligned bundles of polymer chains in the rubbing direction that can further serve as nuclei for oriented growth. To that aim, it is necessary to disentangle polymer chains, in particular in the amorphous zones. This requires enhanced molecular mobility that is obtained by the melting of the soft alkyl side chains (see Figure 6). Films of the larger M_w fractions show more chain entanglements and thus require a higher rubbing temperature to disentangle chains during rubbing.

The HTR alignment method (see Figure 6.i) is indeed very versatile and applicable to a large palette of PSCs. Not only can p-type polymers be aligned, but also alternated donor–acceptor copolymers, e.g. poly{[N,N'-bis(2-octyldodecyl)-1,4,5,8-naphthalene-dicarboximide-2,6-diyl]-alt-5,5'-(2,2'-bithiophene)} (p(NDI2ODT2)). Highly oriented films of p(NDI2OD-T2) can be obtained using T_R=80 °C. When followed by thermal annealing at 280 °C for 1 min, a remarkable dichroic ratio of more than 25 can be reached.[60] From the ED pattern, many very sharp reflections are recorded for p(NDI2OD-T2) after post-rubbing

annealing (see Figure 3) whereas as-rubbed films show only a limited set of arced reflections. Interestingly, annealing at 310 °C after rubbing (T_R= 80 °C) results in a reorientation of the domains on the substrate from “face-on” to “edge-on” together with a structural transition to a different polymorph of the polymer (form I is transformed into form II). Notably, the reorientation of crystalline domains preserves the in-plane direction of the chains imparted by HTR.[60]

The importance of rubbing temperature on the contact plane of the PSC crystals on the substrate was also noticed by Zhong et al. for two alternated copolymers made of the 4,7-bis(4-(2-octyldodecyl)thiophen-2-yl)-5,6-difluorobenzo[c]-[1,2,5]thiadiazole unit with different comonomers: bithiophene in PBT4T and thieno[3,2-b]thiophene (TT) in PDTBT-TT.[71] Very high DRs were obtained for both polymers: DR = 17 for PDTBT-TT (T_R= 220 °C) and DR = 30 for PBT4T (T_R= 200 °C). Electron diffraction demonstrated significant crystallization along with high in-plane orientation induced by HTR. Initially, non-rubbed films show a single Scherrer ring corresponding to the 020 reflection (π-stacking periodicity) indicating that pristine films are made of edge-on crystals with random in-plane orientation. After rubbing at T_R= 200 °C, the PBT4T equatorial h 0 0 reflections (h = 1−4) replace the initial 0 2 0 ring, indicating the transformation of edge-on to face-on crystal orientation. In the case of PDTBT-TT, alignment sets in at T_R= 150 °C for the films of PDTBT-TT rubbed at T_R= 220 °C, ED demonstrates also a coexistence of aligned face-on and edge-on crystals.[71]

Other conjugated polymers used in OPV were also aligned by HTR. For instance, poly[[4,8-bis[(2-ethylhexyl)oxy]benzo[1,2-b:4,5-b’]dithiophene-2,6-diyl-[3-fluoro-2-[2-ethylhexyl) carbonyl]thieno[3,4-b]thiophene-4,6-diyl]], (hereafter PTB7) was aligned with DR in the range 5-6 at T_R= 200 °C.[63] In the case of PTB7, HTR was found to align very well the polymer chains parallel to the rubbing direction but rubbed films display almost no

diffraction peaks suggesting essentially amorphous films made of aligned chains. Combining HTR with an annealing step helped reach DR = 12, but still there was no improvement in the crystallinity of the films. The crucial effect of the solvent used for PTB7 film preparation was identified as was the case for PFO. Changing the solvent from ortho-dichlorobenzene (oDCB) to chloroform helped prepare highly crystalline PTB7 thin films by HTR ($T_R \geq$ 240°C) followed by annealing (T_{ann}= 260°C) for 1h. Numerous reflections including mixed reflections in ED were observed and the analysis of the ED patterns made it possible to propose a structural model for this polymer.[63] Similarly, Fischer et al. managed to combine electron diffraction data from thin films aligned by HTR and single-crystal like data to uncover the structure of Poly(Cyclopentadithiophene-Alt-Benzothiadiazole) with branched side chains.[64]

Table 1. Collection of PSC alignment methods and associated advantages/disadvantages.

Alignment method	Advantages	Disadvantages	References
I.a. Blade coating	- Requires small amounts of polymer solution. - Possibility to tune orientation with translation speed of the blade - Uniform film thickness.	- Multi-parameter technique (temperature, solvent, concentration, speed, substrate). - Strongly dependent on macromolecular parameters and solvent.	16-22
I.b. Brush-coating	- Unique solution-coating approach. - Fast and versatile - Unique tapered film structure when using special brush	- Orientation fully dependent on the deposition region of the polymer film. - Complicated fabrication process leads to high cost. - Difficult to fabricate in a large scale.	23-26
I.c. SVF-HMF	- Contactless alignment method - Possibility of molecular orientation over macroscopic length scale.	- Mostly material-specific. - Requires specific high magnetic field equipment - Limited size and uniformity in film thickness and morphology.	27,28
II.a. Melt-draw method	-Possibility to make ultrathin and freestanding polymer films with high degree of orientation on large scale. -Only two parameters are involved for high orientation (temperature and take-up speed).	- Difficulty to control the Temperature of the film upon pulling - Film thickness is not easy to reproduce	29,30,31
II.b. Strain alignment	- Irrespective of substrates, deposition of polymer film can stimulate optimum morphology. - Contactless oriented film generation - Easy transfer of aligned film to any kind of substrates.	- Limited dichroic ratio - Strong dependence on molecular weight - Potential impurity contamination.	32,33
II.c. Friction-Transfer	- Fast and large scale alignment method - Very high and uniform in-plane orientation - Solid state processing without organic solvents	- Requires substrates that can be heated to the optimal friction transfer temperature - Film thickness is not easy to reproduce - Large amounts of polymer are necessary	34-39
III. Epitaxy	- Effective method to obtain very high crystallinity. - Tuning temperature, crystallization solvent and speed of evaporation can produce high orientation over large surfaces. - complex nanostructurations and orientations are possible	- Fully dependent on the crystalline substrate. - Strong dependence on molecular weight - Limited to lab-scale device fabrication.	43-55
IV High Temperature Rubbing	- Fast and large-scale technique, applicable to multiple substrates - Precise control of polymer orientation and crystallization. - large temperature range (10^0C to 250^0C).	- Optimal rubbing temperature depends on macromolecular parameters - Loss of polymer material upon rubbing	53,59-66

Zheng et al. applied successfully the HTR technique to poly[[2,5-di(2-octyldodecyl)pyrrolo[3,4-c]-pyrrole-1,4(2H,5H)-dione-3,6-diyl]-alt-[2, 2':5', 2'':5'', 2''':5''', 2''''-Quinquethiophene]-5,5''-diyl]] (PDPP-5T).[66] As expected, this polymer showed a strong impact of the molecular weight of alignment by HTR. However, contrary to previous findings for P3HT and C_{12}-PBTTT for which higher T_R is necessary to align polymers of increasing molecular weight, the opposite was observed for PDPP-5T. The best alignment achieved by HTR leads to DR = 5.5 for PDPP5T with medium molecular weight.[65]

B) Orientation of PSCs and fabrication of anisotropic devices

I. Orientation of PSCs in thin films for OFETS

As demonstrated by Hamidi-Sakr et al., HTR is an effective method to tune the semi-crystalline structure of P3HT in oriented thin films.[61] The rubbing temperature can be used as a handle to control in-plane orientation and crystallinity of the P3HT films. Importantly, the crystallinity can be tuned in the range 25-60% for T_R increasing between 50°C and 180°C whereas the order parameter S increases to values as high as 0.83 for T_R= 220°C. Hamid-Sakr et al. measured OFET mobilities in transistors comprising an aligned P3HT layer in Bottom Gate Bottom Contact (BGBC) configuration and without treatment of the SiO_2 surface. The P3HT film was aligned at different rubbing temperatures and the anisotropic charge mobility was measured for the chain oriented parallel and perpendicular to the channel. Regardless of rubbing temperatures, the aligned P3HT films showed a strong anisotropy of charge mobility. Typically $\mu_{//}/\mu_{\perp}$ was found in the range $2 \cdot 10^2 - 2$. The decrease of the anisotropy of mobility with T_R was attributed to the change of the dominant contact plane of P3HT crystals from face-on at low T_R to edge-on for high T_R. Surprisingly, the high values of crystallinity and

orientation achieved for T_R=220°C did not translate in high charge carrier mobilities. The mobility in the chain direction $\mu_{//}$ was found to level at a value of the order of $4 \cdot 10^{-3}$ $cm^2/V \cdot s$ in BGBC OFETs. These low $\mu_{//}$ values were partly attributed to the detrimental effect of amorphous zones interrupting transport paths along the chain direction. The semi-crystalline morphology of rubbed P3HT with an alternation of crystalline and amorphous lamellae is less adapted to large charge mobilities than the oriented fibrillar morphology obtained for solvent casting methods with high boiling point solvents. As for spherulites, the higher transport in the chain direction was attributed to existence of tie-chains bridging amorphous interlamellar zones.

Beside P3HT, HTR was also used to probe the anisotropy of charge transport in OFETs based on rubbed C_{12}-PBTTT films. A strong charge transport anisotropy was measured in rubbed PBTTT thin films with a progressive decrease of the anisotropy $\mu_{//}/\mu_{\perp}$ as the PBTTT crystals changed from face-on to edge-on orientation with increasing T_R.[59] Depending on the annealing conditions after rubbing, this anisotropy of hole mobility could be tuned in the range 7-70 with the highest mobilities along the rubbing direction and the largest anisotropies observed for the oriented face-on PBTTT films. Another PSC, namely polythieno[3,4¬b]¬thiophene¬co-benzodithiophene (PTB7) was also used in BCBG OFETs to measure the anisotropy of charge transport.[63] The best oriented and crystalline PTB7 films showed a dichroic ratio of 12 whereas the hole mobility $\mu_{//}$ was improved by a factor of six in the chain direction as compared to non-oriented spin-coated films ($\mu_{//} = 5.8 \times 10^{-3}$ cm^2 V^{-1} s^{-1} vs $\mu_{\perp} = 3.1 \times 10^{-4}$ cm^2 V^{-1} s^{-1}).

The best results on OFETs based on rubbed thin films were obtained by Tremel et al. for the n-type polymer PNDIT2OD (see Figure 7).[60] Large-scale alignment of PNDIT2OD was achieved by a combination of HTR and thermal annealing with dichroic ratios up to 10 and by

mastering the polymorphism of aligned films. Two polymorphs of P(NDIT2OD-T2) were evidenced and correspond to segregated (form I) and mixed (form II) types of stacking of NDI and T2 blocks (Figure 7.a). This typical polymorphism is easily evidenced by analyzing the UV-vis absorption spectra of the films *versus* annealing temperature (Figure 7.b). The polymorphism of P(NDIT2OD-T2) was found to impact strongly the charge transport properties in oriented films. As-rubbed films showed rather poor charge mobilities with $\mu_{//}$=3x10^{-3} cm^2/V·s and $\mu_{\perp}$ =5x10^{-4} cm^2/V·s. In strong contrast, thermal annealing in the range 220°C-310°C improved crystallinity and orientation as well as electron mobilities. Highly oriented P(NDIT2OD-T2) films of form II were obtained after annealing the films at 310°C and probed as OFET layers for anisotropic in-plane charge transport. Top-gate Top Contact (TGTC) transistors showed high electron mobilities of up to 0.08 cm ^{2} V $^{-1}$ s $^{-1}$ in the chain direction, which was up to 10 times higher than mobilities perpendicular to the polymer chain. As compared to non-oriented films, the HTR-aligned and annealed films showed a 3-5 fold increase of charge mobility in the chain direction (Figure 7.c and 7.d). This result underlines the importance of mastering both i) polymorphism and in-plane orientation of the active layer as well as ii) the device architecture (top-gate *versus* bottom-gate) to achieve large charge mobilities in OFETs made of rubbed PSC layers.

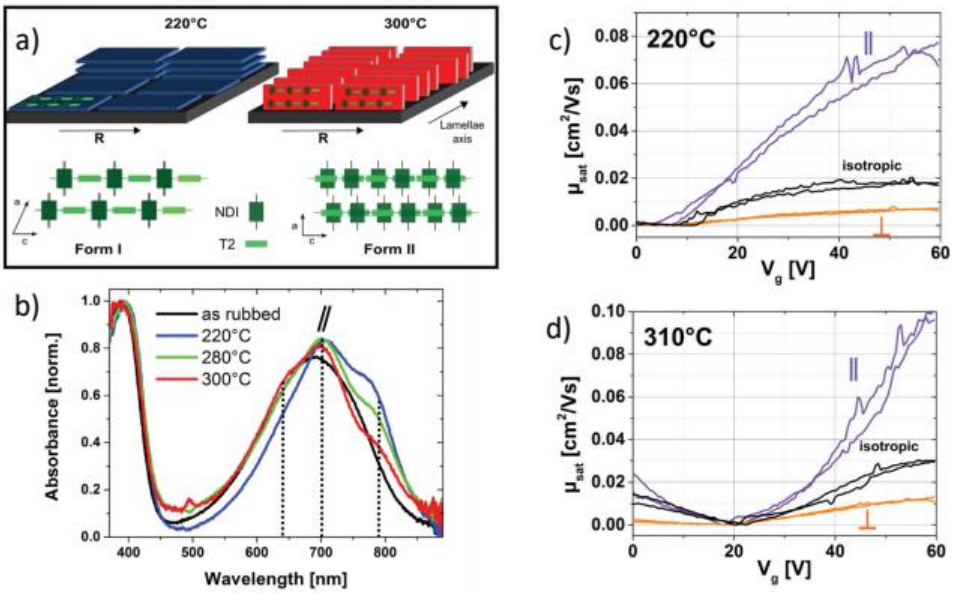

***Figure 7**. Polymorphism (a) and UV-vis absorption (b) of the form I and form II P(NDIT2OD-T2) thin films rubbed at 80°C as a function of thermal annealing. When films are annealed at 300°C, they convert to form II (mixed type of stacking). c) and d) Mobility measurements versus gate voltage V_g of non-oriented and oriented P(NDIT2OD-T2) thin films corresponding to form I after annealing at 220°C (c) and to form II obtained for annealing at 310°C (d). Mobilities are measured in the directions parallel ($\mu_{//}$) and perpendicular ($\mu_{\perp}$) to the rubbing direction. Adapted with permission from reference 60.*

II. Application of high temperature rubbing to the preparation of electronic devices (solar cells, photodetector applications and light modulators).

Organic solar cells fabricated through alignment by rubbing were first reported by Vohra et al.[72] They demonstrated that the photovoltaic properties of solar cells were enhanced by rubbing the P3HT films prior to $PC_{60}BM$ deposition. Compared to the unrubbed P3HT films, i) rubbed P3HT polymers were less dissolved during the $PC_{60}BM$ deposition, ii) $PC_{60}BM$ molecules diffused better into rubbed P3HT polymer matrix, and iii) rubbing P3HT film displayed a reorientation of the crystallites from edge-on to face-on configuration, resulting in a better charge transport along the vertical direction in the solar cell. Therefore, the

graded bilayer solar cells based on rubbed P3HT showed higher photovoltaic performances. Such oriented photovoltaic layers were used as polarizing organic photovoltaic devices (ZOPV) to improve the energy efficiency in liquid crystal displays (LCD).[73] ZOPV devices were designed by Yang and co-workers to be integrated into LC displays playing the twofold role of light polarizer and photovoltaic (PV) device. ZOPC devices were prepared by using oriented P3HT films prepared by HTR and showing a high DR (Figure 8.a-b). Then, a $PC_{60}BM$ acceptor layer was deposited atop the rubbed P3HT films. Incidentally, the evaporated $PC_{60}BM$ layer helped to fill most cracks created by the mechanical rubbing, avoiding short circuits in the P3HT/ $PC_{60}BM$ solar cell. Polarized UV-vis spectroscopy demonstrated that the diffusion of $PC_{60}BM$ molecules into P3HT affected neither the P3HT molecular orientation nor the packing of P3HT chains. The quasi-bilayer films showed a high DR of approximately 11.3 at 604 nm. These ZOPV devices based on the inverted quasi-bilayer structure (Figure 8.c) showed a dichroic photovoltaic effect with a J^{sc} ratio $J^{SC}_{//}/J^{SC}_{\perp}$ of 3.54 (Figure 8.d). As a result, over 10% of the ideal energy recycling efficiency by ZOPV devices was performed in LCD.

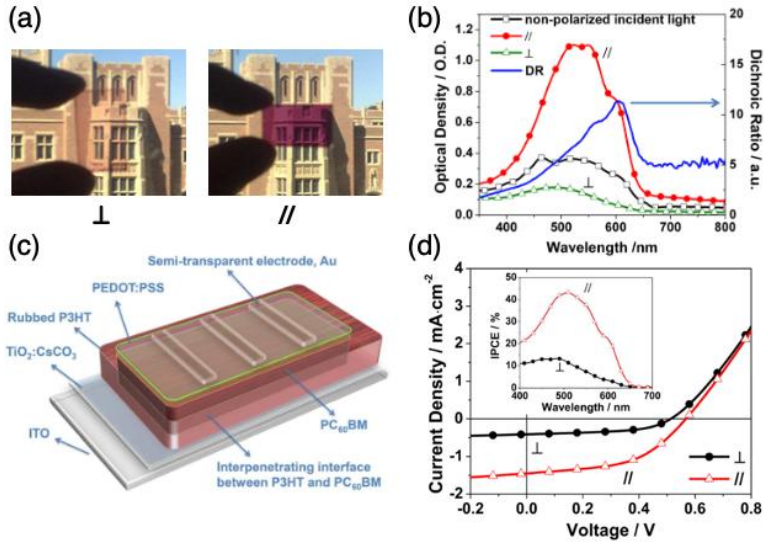

***Figure 8**. (a) Images of an oriented P3HT film with the rubbing direction perpendicular (⊥) and parallel (//) to the light polarization. (b) Polarized UV-visible absorption spectra of quasi-bilayer P3HT-$PC_{60}BM$. The incident light polarization is parallel (//) or perpendicular (⊥) to the rubbing direction. The dichroic ratio (DR) can be determined by measuring the absorbance in two directions as a function of wavelength ($DR= Abs_{//} / Abs_{\perp}$). (c) ZOPV device structure based on the inverted quasi-bilayer. (d) Dichroic J-V characterization of ZOPV device in (c). The intensity of polarized incident light is around 33 mW/cm2. Inset: polarized IPCE spectra. Reproduced with permission from reference 73.*

Recently, the group of O'Connor reported a record in-plane alignment of bulk heterojunction films used in polarization sensitive photodetectors.[74] In such devices, the incident light polarization is converted to an electrical signal that can be measured. The key factors for polarization sensitive photodetectors are i) photocurrent anisotropy and ii) electrical responsivity upon illumination. The authors focused on the bulk heterojunction composed of Poly(benzodithiophene-alt-dithienyl difluorobenzotriazole) (PBnDT-FTAZ) and poly {[N, N'-bis(2-octyldodecyl)-1,4,5,8-naphthalenedicarboximide-2,6-diyl]-alt-5,5'-(2,2'-bithiophene)} P(NDI2OD-T2), also known as N2200 (Figure 9). The two semiconducting polymers have i) a complementary spectral absorption; ii) a high thermal stability as well as adapted thermomechanical properties for rubbing. The film alignment was significantly enhanced after thermal annealing of the rubbed blend films (Figure 9.b,c). The maximum DR with low M_w polymers reached nearly 17 using HTR at T_R=160°C and a thermal annealing step at 275°C (5 min). Semi-transparent organic photodiodes based on the well-aligned films were fabricated with an inverted organic photovoltaic architecture. (Figure 9.d) A high dichroic photovoltaic effect was observed. (Figure 9.e) The spectral responsivity indicated that

detectors have a large photocurrent ratio of 15 while maintaining responsivity above 20 mA/W, operating in a self-powered regime.

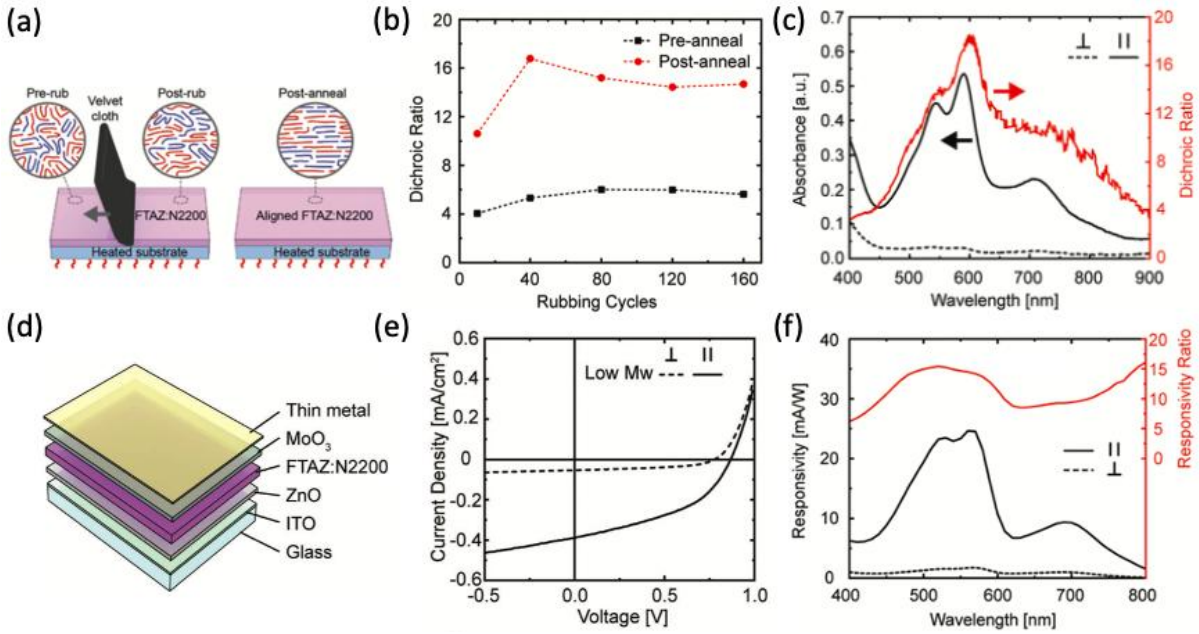

Figure 9. *(a) Schematic illustration of FTAZ-N2200 polymers blend alignment procedure. (b) The DR at a wavelength of 595nm as a function of rubbing cycles for pre-annealed and post-annealed FTAZ-N2200 blend films. (c) Polarized UV-visible absorption spectra and the corresponding DR for aligned (40 rubbing cycles) and annealed films (at 275°C for 5 min) with the rubbing direction parallel (//) and perpendicular (⊥) to the incident light polarization. (d) Polarization sensitive photodiode detector device structure. (e) J-V characteristics for photodiode detector device under optimal alignment conditions. (f) Responsivity and responsivity ratio of polarizing photodiode detector (e) for parallel and perpendicular incident light polarization. Reproduced with permission from reference 74.*

Another innovative application of mechanical rubbing of PSCs and PCs was introduced by the group of Heiser et al. to design a new self-powered switchable glazing, named Photovoltaic Spatial Light Modulator (PSLM). The principle of such devices is

illustrated in Figure 10. A PSLM can be divided in two parts: I) a liquid crystal light valve that modulates the optical properties, and II) an organic photovoltaic unit (PVU) capable of generating a voltage upon illumination. The latter allows the device to operate in a self-powered regime. (76) As illustrated in Figure 10, this device consists of a twisted nematic liquid crystal, sandwiched between two ITO substrates coated with alignment layers. The alignment layers are mutually perpendicular, enabling the LC molecules to twist by 90° between the two sides. The PVU is positioned between the LC layer and one of the ITO substrates. It includes a hole transporting layer (HTL), a bulk heterojunction (BHJ) and an electron transporting layer (ETL). The BHJ is composed of electron-donor and electron-acceptor organic semiconducting materials, that can absorb the incident photon and generate free charge carriers (i.e., electrons and holes). Then, the electrons and holes reach the ETL and HTL respectively, creating a voltage drop across the multilayer stack referred to as photovoltage (V_{ph}). One of the alignment layers is produced by directly rubbing the HTL such as PEDOT:PSS in contact with the LC layer or by adding an oriented polymer layer on top of the HTL e.g., a rubbed P3HT layer.

As depicted in Figure 10.a, the PSLM device operates between crossed polarizer and analyzer. The incident light is linearly polarized by the polarizer. In the open-circuit condition (OFF state or clear state), photogenerated holes and electrons accumulate in the HTL and ETL, respectively. No electric field is produced across the LC layer. Consequently, the light polarization is rotated 90° by the LC molecules, passing through the analyzer that is perpendicular to the initial polarizer. This leads to a transparent state. In the case of short-circuit (ON state or dark state), both ITO substrates are connected in series, as shown in Figure 10.b. The electrons can be transferred to the opposite ITO substrate. The voltage drops across the LC layer, that matches roughly the photovoltage delivered by the BHJ layer.

If the photovoltage exceeds the Frédericksz transition voltage (V_{th}), the LC molecules start to change orientation, from the twisted state to the homeotropic state. In this case, the light polarization cannot be rotated by 90° and is blocked by the analyzer, resulting in a decrease of the device transmittance.[76] Since the photovoltage amplitude is influenced by local light intensity, the device response is spatially resolved.

Most relevant for this review is the fact that thin films of rubbed PSC such as P3HT can be used as LC alignment layers in the PSLMs. It is well known that gently rubbed P3HT polymers yield a high-quality LC alignment.[75] Going one step further, the anisotropic optical PV layers as described previously in this section could be integrated into such PSLMs to avoid the use of external polarizers and thereby improving the transparency of devices in the OFF state.

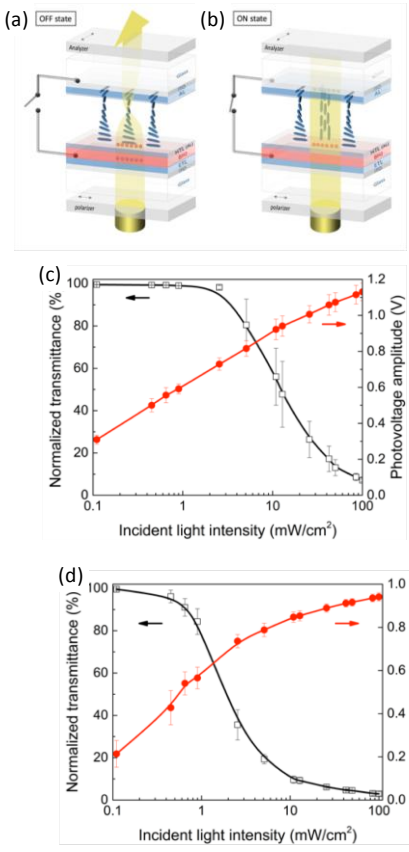

***Figure 10**. Scheme illustrating the working principle of a Photovoltaic Spatial Light Modulator (PSLM) in the (a) OFF state and (b) ON state. (c) Normalized transmittance (black line), measured in the ON state, and photovoltage amplitude (red line), measured in the OFFs state, of a Photovoltaic Spatial Light Modulator devices versus incident light intensity for a P3HT:ICBA tandem structure (c) and a PM6:ICBA single junctions (d). In both cases, the error bars correspond to confidence intervals of 90%. Reproduced with permission from reference 75.*

C) Fabrication of oriented conducting polymer films.

Shirakawa and coworkers reported for the first time in 1977 the possibility to fabricate highly conducting polymers by doping conjugated polymer such as polyacetylene.[77] This remarkable discovery initiated an extensive and systematic research on conducting polymers such as poly(diacetylene) or polyaniline doped by redox or acid-base approaches.[78,79] Conducting polymers were widely used in organic electronic devices and thermoelectric application.[80-84] However, as compared to PSCs, most conducting polymers show high levels of disorder due in part to the random distribution of dopant molecules in the polymer matrix.[85-88] Structural disorder of "classical" conducting polymer has been a serious limitation for the efficiency of charge transport in these materials. There are several strategies to improve order in CPs to reach better transport properties. First, alignment of semiconducting and conducting polymer is an effective method to improve charge transport due to the intrinsically anisotropic transport in these polymers. As an example, stretch-aligned polyacetylene (PA) doped with iodine showed very high electrical conductivities in the 10^4-10^5 S.cm^{-1} range.[89,90] However, PA is not stable in ambient and can only be processed in the form of a few tens of microns thick films that are difficult to use in the

fabrication of TE devices.[84,91] Therefore, alternative conjugated polymers such as polythiophenes with better stability and facile processing using solution-based coating methods have been widely explored. The beneficial effect of orientation on charge transport in sequentially doped P3HT polymers has been recently illustrated by Hamidi-Sakr et al. [92] Highly oriented conducting polymer films were prepared by combining high temperature rubbing of RR P3HT and a soft doping of aligned films using spin-coating of a dopant solution, as shown in figure 11.a. The polarized UV-vis-NIR spectra show highly polarized polaronic absorption bands (P1, P2) of P3HT for POL//R as well as polarized absorption bands of F_4TCNQ^- anions for POL⊥R. The experimental results suggested that F_4TCNQ^- anions are oriented with their molecular long axis perpendicular to the P3HT chain direction. More importantly, the F_4TCNQ doping maintains fully the in-plane orientation of the original rubbed P3HT films. Doping impacts the crystal structure of P3HT. Electron diffraction shows that incorporation of F_4TCNQ^- in the layers of alkyl side chains results in a slightly expanded unit cell along side chains and a reduced π-stacking distance (Figure 11.c, d). It was also observed that both charge conductivity (σ =22±5 $S.cm^{-1}$) and Seebeck coefficient (S =60±2 $\mu V. K^{-1}$) are enhanced along the rubbing direction. Therefore, doping of aligned semi-conducting polymers was found to be an effective method to fabricate conducting polymers films and an interesting alternative to other methods to align directly conducting polymers such as PEDOT:PSS.[93] Indeed, strain-alignment of PEDOT causes unwanted rupturing of the films with increasing strain. This is related to the very rigid and limited thermomechanical properties of PEDOT:PSS. Accordingly, in the next section, we will review some typical sequential doping methods used to control effectively the carrier density and conductivity of doped PSC films. Representative thermoelectric properties such as charge conductivity, Seebeck coefficient and power factors for different doping methods are collected in Table 2.

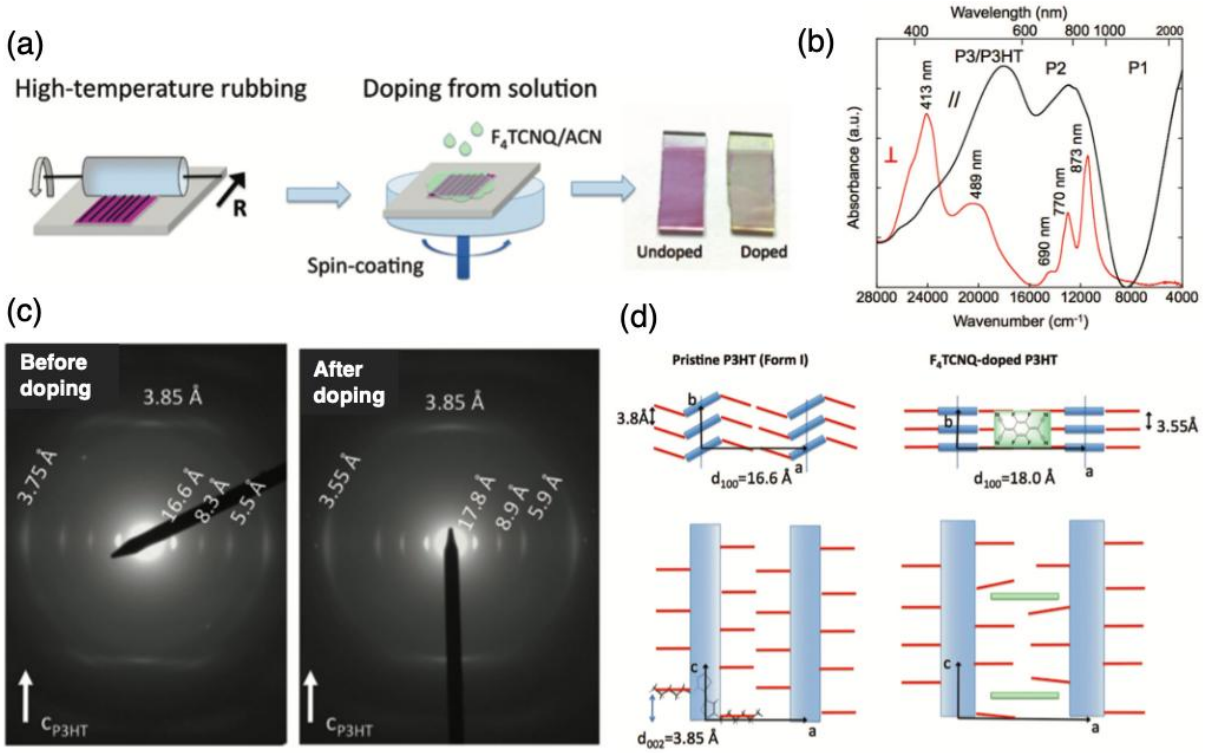

Figure 11. *(a) Schematic illustration of two-step preparation method for highly oriented conducting polymers. First, the P3HT films were first aligned by high temperature rubbing. R is the rubbing direction. Second, aligned films were doped with a solution of F_4TCNQ in acetonitrile. The picture on the right in (a) shows the color change of the films before and after doping. (b) Polarized UV-vis-IR absorption spectra for highly oriented and doped P3HT films for incident light polarization parallel (//) and perpendicular (⊥) to the rubbing direction. (c) Structural evolution of oriented P3HT films doped with F_4TCNQ as obtained by low dose TEM. Electron diffraction patterns of undoped P3HT films (left) and of the doped films (right) (d) Schematic illustration of the crystal structure of pristine and doped P3HT. Reproduced and adapted from reference 92.*

I. Doping methods.

The electrical and thermoelectric (TE) performance of conductive polymers can be optimized by improving the level of order in the organic thin films. The nanostructure of doped films depends on the conjugated polymer configuration (molecular weight, regioregularity), dopant size, processing solvent and specific doping methods. Several groups have shown that various doping methods result in different morphologies of doped polymers. Differences in electrical conductivities by 1~2 orders of magnitude were observed.[94-97] Therefore, it is crucial to understand how doping methods impact the interaction of the host semiconducting polymer with the dopants, charge transport properties and TE properties. Doping methods can be classified as i) mixed doping, ii) sequential doping (SqD) and iii) electrochemical doping (Figure 12). In SqD, the dopant molecules have been inserted into the semiconducting polymer matrix by various approaches including spin coating, dipping or thermal evaporation. Let us briefly review these three doping methods.

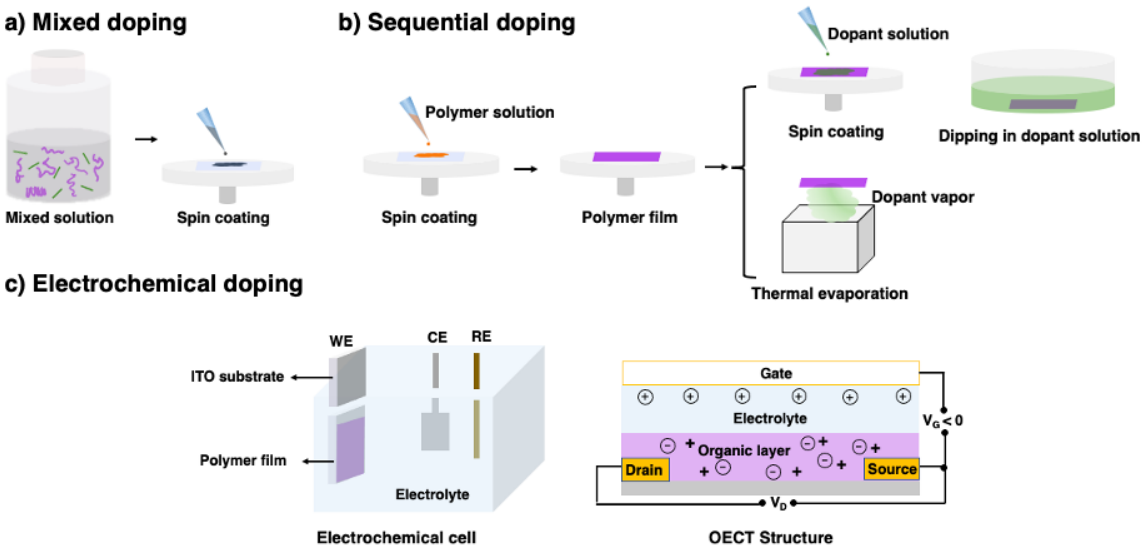

***Figure 12**. Schematic illustration of various doping methods of PSCs: a) Mixed solution doping; b) Sequential doping; c) Electrochemical doping using an classical electrochemical cell or an Organic Electrochemical Transistor (OECT) device. WE is the working electrode, CE is the counter electrode and RE is the reference electrode*.

1.1 Mixed solution doping

Mixed doping is a simple and effective way to prepare conducting polymers. Both the conjugated polymer and the dopant are mixed in a common solvent and the blend is deposited on substrates to form doped thin films (Figure 12.a). This approach has been used by Aziz at al. to dope P3HT with F_4TCNQ.[98] The films prepared from F_4TCNQ-P3HT blend solutions exhibit a conductivity of 1 $S{\cdot}cm^{-1}$, which is 5 orders of magnitude higher than that of the undoped pristine P3HT film. The impact of F_4TCNQ doping concentration on the doping efficiency and conductivity was investigated by Duong et al.[99] Their results indicate that the doping efficiency and the electrical conductivity in the strong doping regime are much higher than in the weak doping regime. The author assigned the increase of conductivity in the strong doping regime to enhanced charge dissociation and carrier generation by the incorporation of dopants into crystalline domains of P3HT. However, mixed doping often reduces drastically the solubility of polymers and doped agglomerates are formed due to the high polarity of the charged complexes, making it difficult to fabricate high-quality and uniform films.[100] In order to improve the quality of the films, blend solutions were prepared at high temperature. However, despite a smooth morphology, a poor doping efficiency was observed for F_4TCNQ-P3HT films spin cast at 80°C.[101] In general, the electrical conductivity is limited due to poor interconnections between crystallites.[94] Alternatively, Sequential doping (SqD) was proposed to yield homogenous doped films.

1.2 Sequential doping

Sequential doping (SqD) has been used to fabricate high-quality conducting polymer films. In SqD, the semiconducting polymer is deposited first on a substrate. Doping is performed in a second step by using dopants in an orthogonal solvent or by depositing the dopants via thermal evaporation (Figure 12.b). The dopant molecules can thus infiltrate a

highly ordered polymer film without modifying the film nanostructure. The doping level of the polymer films is easily tuned by varying the doping concentration. Scholes et al. demonstrated that SqD is an effective technique to create heavily doped pristine-quality films of P3HT with the molecular dopant F_4TCNQ.[100] The films prepared by sequential solution processing are more uniform and flatter than those prepared by mixed doping. 2D-GIWAX showed the F_4TCNQ dopant molecules intercalate into P3HT films preserving the preferentially edge-on crystal orientation and much of the overall crystallinity found in undoped polymer films. Moreover, Jacob et al. demonstrated that the film morphology is improved by SqD due to a larger number of interconnections between P3HT crystals via tie-chains. As a consequence, charge conductivities are improved by a factor of 3 to 15 as compared to those obtained for films prepared by mixed doping.[94] A high charge conductivity of 12.7 $S.cm^{-1}$ for vapor-phase doped P3HT was reported by Hynynen et al. [95] The F_4TCNQ molecules were thermally evaporated on the top of pure P3HT films, inducing a solid-state diffusion from the surface into the bulk films without changing the nanostructure of the polymer. The doping level can be controlled by the evaporation time. Structural investigations indicated that vapor phase doping of P3HT films led to the increase of the lamellar stacking periodicity d_{100} and to the decrease of the π-stacking distance, suggesting the incorporation of F_4TCNQ into alkyl side chain layers of P3HT. Importantly, the crystallinity of undoped films determines the electrical conductivity of doped films. Regarding the polymer C_{14}-PBTTT, vapor phase doping produced also films with a higher conductivity and power factor than films produced by mixed doping.[97] Chabinyc and co-workers used polarized resonant soft X-ray scattering (RSoXS) to determine the length scale of molecular ordering in the doped films. More precisely, the backbone alignment is quantified by the orientational correlation length (OCL), which is proportional to the charge mobility. Vapor

phase doped films display an OCL larger by a factor of ~ 5 than films prepared by mixed doping. In addition, very high conductivities of ~670 $S.cm^{-1}$ as well as large thermoelectric power factors (PF) of ~120 $\mu W.m^{-1}.K^{-2}$ were obtained.

A variation of SqD was developed by Vijayakumar et al. for highly aligned C_{12}-PBTTT thin films and extended to P3HT by Untilova et al.[102,103] The orientation of semiconducting polymer films was performed before doping. The improved SqD process is called Incremental Concentration Doping (ICD).[102] In ICD, the oriented films are doped by successive dipping in dopant solutions of increasing concentration whereas in the direct doping (DD) the rubbed films are dipped only once in a solution at a given doping concentration. The influence of SqD methods (ICD and DD) on the charge conductivity and on the power factor (PF) of poly(2,5-bis(3-dodecyl-2-thienyl) thieno[3,2-b] thiophene) (C_{12}-PBTTT) films doped with F_4TCNQ and 1,3,4,5,7,8-hexafluoro-tetracyanonaphthoquinodimethane (F_6TCNNQ)[104] has been studied. The results show that both of ICD and DD methods maintain the alignment in rubbed C_{12}-PBTTT films, enabling the fabrication of oriented conductive polymers with highly anisotropic optical and electrical properties. The authors demonstrated that ICD produces higher electrical conductivity and larger thermoelectrical power factor (PF) than DD for doped C_{12}-PBTTT films by preserving the high degree of order of undoped pristine polymers (see Figure 13). The higher conductivities for ICD films were attributed to higher charge mobilities since the pristine structure of the films is conserved in the ICD method. Doping of C_{12}-PBTTT films with F_6TCNNQ through the ICD method results in electrical conductivities up to 2400 $S.cm^{-1}$ and PF of approximately 530 $\mu W.m^{-1}.K^{-2}$. A comparative study on the charge conductivities in oriented P3HT films doped with F_4TCNQ using ICD and DD was recently

reported by Untilova et al.[103] Similarly to C_{12}-PBTTT, ICD enhances the charge conductivity in doped thin films over DD by a factor 1.5.

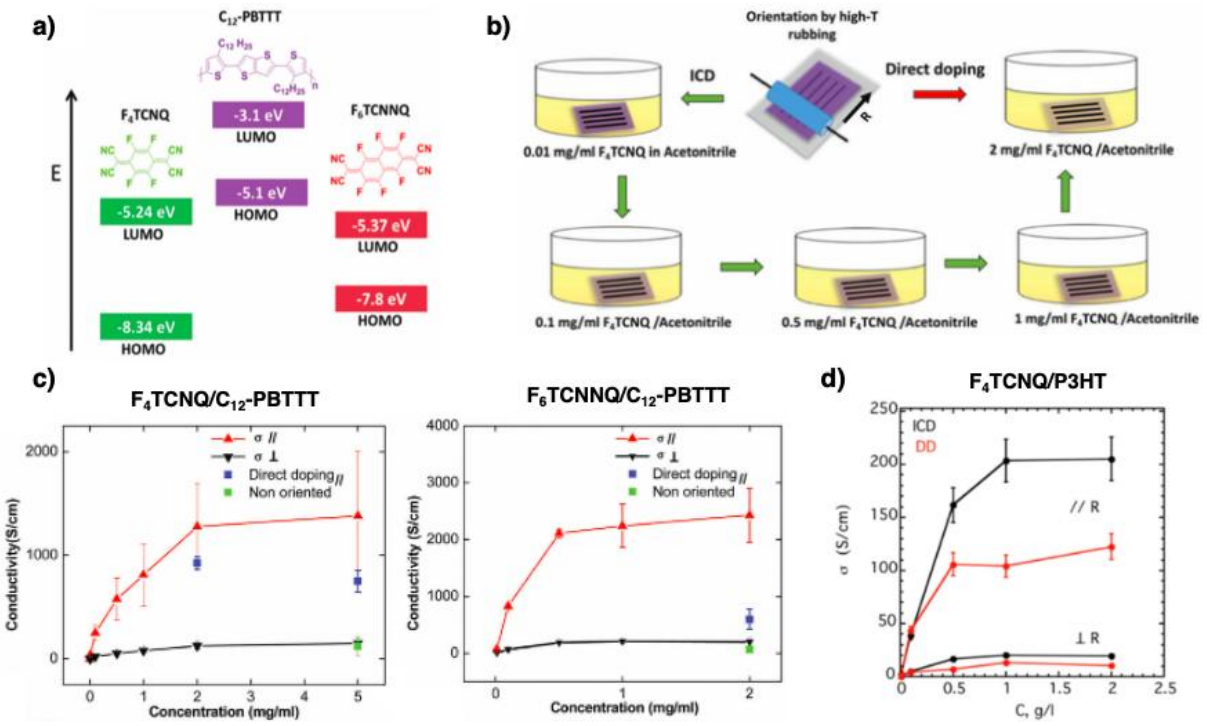

Figure 13. *a) Energy diagram of the LUMO and HOMO levels of F_4TCNQ, C_{12}-PBTTT and F_6TCNNQ. b) Schematic illustration of the method of preparation of oriented and doped PSC films using either direct doping (DD) or Incremental Concentration Doping (ICD). c) and d) Evolution of the charge conductivity in oriented C_{12}-PBTTT films as a function of increasing doping concentration of F_4TCNQ (c) and F_6TCNNQ (d). The charge conductivity of samples doped by ICD are measured parallel (red) and perpendicular (black) to the rubbing directions. The blue dots correspond to the conductivities of DD films at high doping concentration measured along the rubbing direction. The conductivity of unrubbed films (green) was measured at maximum doping concentration using the ICD method. d) Evolution of the charge conductivity in oriented P3HT films as a function of increasing F_4TCNQ doping*

concentration using two doping methods: DD and ICD. Reproduced and adapted from references 102 and 103.

Table 2. Collection of reported thermoelectric properties of oriented conjugated polymer films doped using various doping methods and comparison with those of non-oriented films.

Semi-conducting polymer	Dopant	Doping method	σ (S.cm^{-1})	α (µV. K^{-1})	$\sigma . \alpha^2$ (µW.m^{-1}. K^{-2})	Reference
P3HT	F_4TCNQ	Mixed solution doping	1.0			98
	F_4TCNQ		1.8			99,101
	F_4TCNQ		8.0			94
	F_6TCNNQ		7			104
	F_4TCNQ	SqD	5.5			100
	F_4TCNQ		3.0			94
PBTTT-C_{12}	F_6TCNNQ	ICD	130±50	45±2	27±13	69
PBTTT-^{8}O	F_6TCNNQ		1100±200	10±1	25±4	
P3HT	F_4TCNQ	Vapor phase doping	12.7±2.8	46±2	2.7	95
PBTTT-C_{14} On untreated quartz substrates	F_4TCNQ		220.00±0.02	39±5	32±9	97
	F_2TCNQ		36±3	140±20	70±20	
PBTTT-C_{14} On an OTS-treaded substrate*	F_4TCNQ		670±4	42±6	120±30	

Oriented P3HT	F_4TCNQ	DD	22±5	60±2	~8.5	92
	F_4TCNQ	DD	122			108
	F_4TCNQ	ICD	287		73±5	
	F_6TCNNQ	ICD	521		79±30	
	$FeCl_3$	ICD	570±100	5.4±0.5	21±6	91
	$Mo(tfdCOCF_3)_3$	DD	509±51	56±2	160±27	110
	Magic blue (MB)	ICD	3460 ± 300	22	171	107
Oriented PBTTT-C_{12}	F_4TCNQ	DD	920±60	57±3	300±20	102
	F_4TCNQ	ICD	1380±700	50.7±4	355±200	
	F_6TCNNQ	DD	600±200	64.5±3	247±74	
	F_6TCNNQ	ICD	2430±500	47±4	530±200	
	$FeCl_3$	ICD	(2.2±0.5) $\times10^5$	9.4±0.5	1994±626	
Oriented PBTTT-^{8}O	F_6TCNNQ	ICD	(5±2) $\times10^4$	24±2	2900±1600	69

*On an octadecyltrichlorosilane(OTS)-treaded substrate

*For oriented films, all the reported values are measured along the rubbing direction

1.3 Electrochemical doping method

The electrochemical doping is a reversible process that can transform a PSC deposited on a conducting electrode into a conducting polymer. Typically, electrochemical doping is carried out in a three-electrode electrochemical cell composed of: i) the conjugated polymers

deposited on an electrode substrate, ii) a platinum grid used as a counter electrode and iii) a reference electrode such as Ag/AgCl. An alternative to this setup is to use a so-called Organic Electrochemical Transistor (Figure 12.c) that allows to measure transport properties upon electrochemical doping of the PSC layer. The potential between the conjugated polymer and the electrode is modulated to oxidize (p-type doping) or reduce (n-type doping) the conjugated polymer (Figure 12.c). Upon oxidation/reduction, counterions of the electrolyte diffuse into the bulk polymer film. The doping level and charge carrier density in conjugated polymer can be accurately controlled by varying the applied voltage.

A study on different oxidized states of P3HT through electrochemical doping has been reported by Enengl et al.[105] The formation of polarons at low doping level and the presence of bipolarons at high doping level was evidenced. Electrochemical doping of P3HT films with different crystallinities was performed by Ludwigs and coworkers.[106] Two deposition methods of the PSCs were considered: i) direct electropolymerisation of monomers that results in rather amorphous PSC films; ii) solution deposition of chemically synthesized P3HT polymers. Their results demonstrate that the P3HT film preparation conditions can alter morphologies ranging from amorphous to highly crystalline films, which has a strong impact on the spectroelectrochemical behavior and HOMO energy level. Recently, Ludwigs et al. reported the preparation of highly conducting P3HT films by electrochemical doping.[107] Despite low crystallinity, the electrochemical oxidation of poorly ordered P3HT films provided a high conductivity of up to 224 $S.cm^{-1}$. In strong contrast, doping of regiorandom P3HT films led to a lower conductivity of 10 S/cm. The high conductivities reached in electrochemically doped P3HT were explained by the coexistence of different redox states of the PSC corresponding to polarons and bipolarons.

II. Impact of doping on the structure of PSC films oriented by rubbing.

II.a. Structure of doped PSCs.

The original work By Hamidi-Sakr showing that F_4TCNQ doping of aligned P3HT preserves structure despite dopant introduction in the crystal lattice of P3HT was an incentive to perform a systematic investigation of the structure of doped-PSCs.[92] In this section, we provide a short overview of various structures formed when dopants enter the lattice of PSCs. We further investigate how the structural changes induced by doping impact charge transport and thermoelectric properties in doped PSCs. The present review focuses essentially on p-type polythiophenes (P3HT, PBTTT) and different dopants (F_4TCNQ, F_6TCNNQ, $FeCl_3$, $Mo(tfd\text{-}COF_3)_3$ and Magic Blue) having different Lowest Unoccupied Molecular Orbital (LUMO) values (Figure 14).

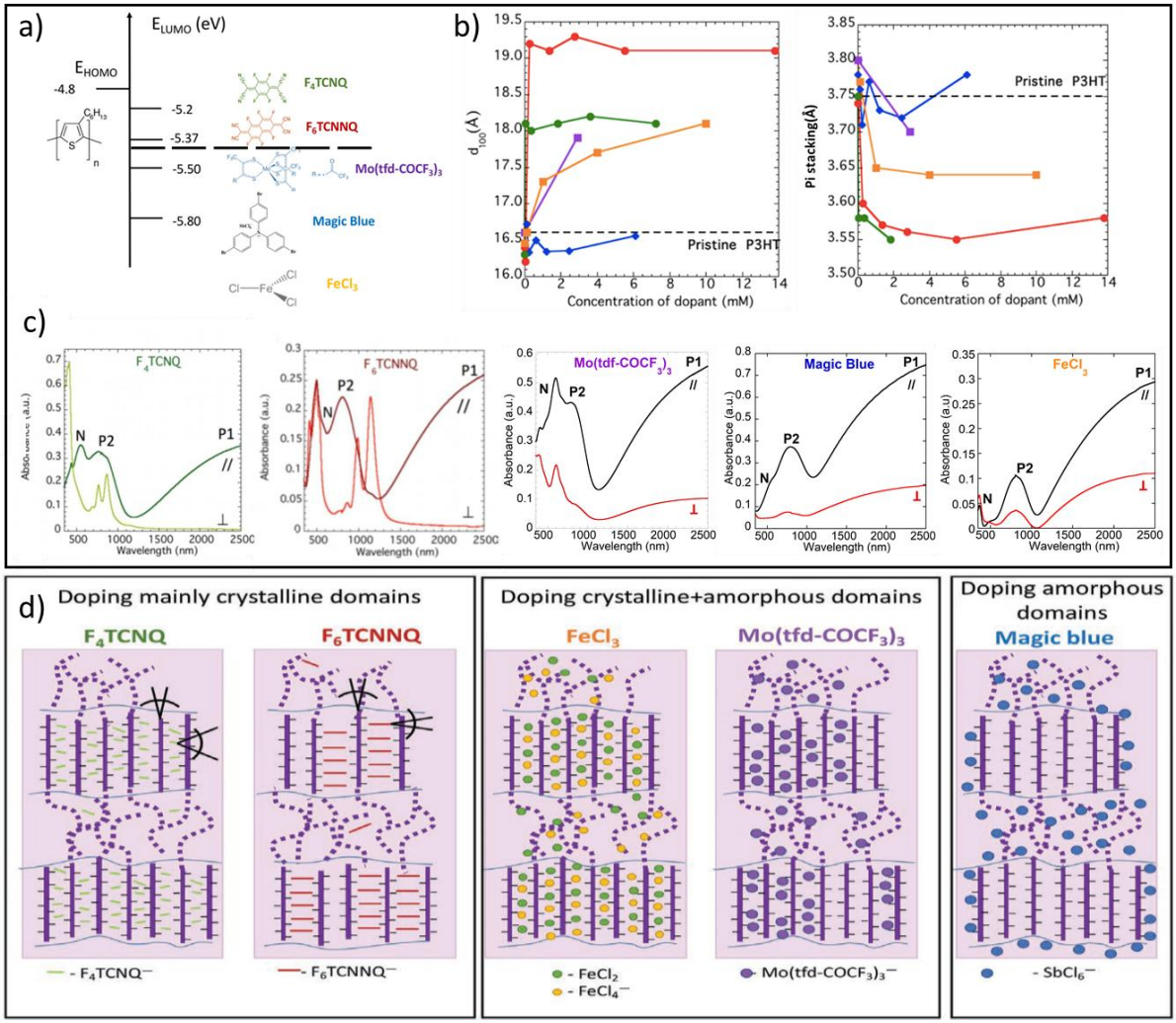

Figure 14. *a) Energy diagram of the LUMO levels and molecular structure of different dopants with respect to HOMO level of P3HT polymer, b) Evolution of the layer spacing along the alkyl side chain direction d_{100} and the π-stacking periodicity d_{020} as a function of the dopant concentration for different dopants. The dotted lines highlight the values of the layer spacings d_{100} and d_{020} of undoped P3HT. c) Polarized UV–Vis–NIR absorption spectra of oriented P3HT polymer films for different dopants plotted against different dopant concentrations for the light polarized parallel and perpendicular to the rubbing direction. The spectra show the polaronic bands P1 and P2 of the doped P3HT and the neutral P3HT peak N*. d) *Schematic representation of various doped P3HT microstructures: doping of the crystalline domains for F_4TCNQ and F_6TCNNQ; doping of both crystalline and amorphous zones for $FeCl_3$ and Mo(tdf-$COCF_3$)$_3$ and doping of the amorphous zones for MB. Reproduced from reference 108.*

Insight into dopant location and organization in the PSC matrix was mainly obtained by the combination of Transmission electron microscopy (low dose diffraction) and polarized UV-Vis-NIR spectroscopy.[108] Interestingly, the investigations showed that sequential solution doping of aligned PSC films can result in different locations of dopant molecules in the semi-crystalline structure of PSCs: i) dopants like F_4TCNQ and F_6TCNNQ locate essentially in the crystals of P3HT, ii) dopants like $FeCl_3$ or Mo(tdf-$COCF_3$)$_3$ are present in the amorphous and crystalline phases of P3HT and iii) the dopant magic blue is essentially located in the amorphous phase of P3HT. Let us review these different cases (see Figure 14).

II.a. Structural changes in sequentially doped P3HT.

A detailed structural analysis of doped and aligned P3HT was performed by Untilova et al. on F_6TCNNQ-doped P3HT. The starting structure of the aligned P3HT films is form I of P3HT as identified by Kayunkid et al.[54] In this structure, 3-hexyl side chains are not interdigitated but form a rather dense packing with some disorder as indicated by the ED patterns (see Figure 15).[54]

For F_4TCNQ doped P3HT thin film, Untilova et al. observed an expansion of the unit cell along the side chain direction from 16.4 Å to 18.1 Å and the contraction of the lattice along the π-stacking direction (from 3.8 Å to 3.6 Å).[92, 109] These results suggest intercalation of F_4TCNQ dopants in P3HT crystals. UV-Vis-NIR spectroscopy demonstrates that F_4TCNQ orients in a plane perpendicular to the polythiophene backbones. Similar observations were made when aligned P3HT is doped with the larger and stronger acceptor F_6TCNNQ. For F_6TCNNQ doped P3HT, electron diffraction (ED) indicates an expansion of the crystal lattice along the side chain from 16.4 Å to 19.2 Å which is higher than for F_4TCNQ. The contraction of the π-stacking distance from 3.8 Å to 3.55-3.60 Å is similar for both dopants. Interestingly, the structure of F_6TCNNQ-doped P3HT reveals additional reflections (see Figure 15.e). The analysis of this ED pattern helped the authors to propose a structural model for F_6TCNNQ-doped P3HT (see Figure 15). The refined structure of P3HT:F_6TCNNQ reminds the "tunnel" structure of iodine doped P3HT reported by Tashiro et al. [110] Structural modeling of iodine doped P3HT indicates that the orientation of polyiodide chains is along the **b** axis of P3HT. the refined structure of P3HT doped with F_6TCNNQ, the long axes of two dopants are oriented along the side chain direction (**a** axis) as shown in figure 15. This indicates that F_6TCNNQ dopant is intercalated in a more ordered manner in P3HT crystal lattice than F_4TCNQ resulting in larger charge conductivities for F_6TCNNQ. The thermoelectric power factors remained almost the same for both dopants, in the 70−80 μW m^{-1} K^{-2} range.[108]

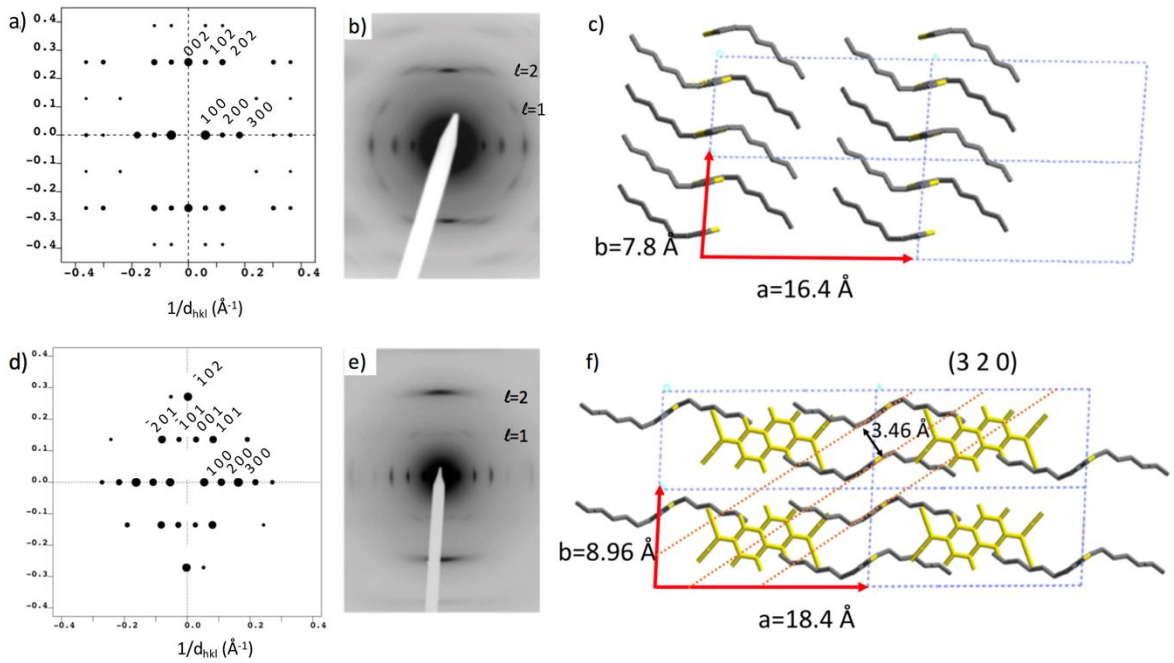

***Figure 15**. Calculated (a and d) and experimental (b and e) electron diffraction patterns for the [0 1 0] zone for P3HT (form I) (a and b) and P3HT-F_6TCNNQ (d and e). The form I structure is taken from reference 53 whereas the doped P3HT structure is refined and corresponds to the model illustrated in Figure 6. In c) and f), the c-axis projection of the pristine and doped structures are shown, respectively. Reproduced from reference 109.*

Sequential doping of P3HT with $FeCl_3$ and Mo(tdf-$COF_3)_3$) leads to a different situation.[111] TEM and polarized UV-vis-NIR show that these two strong oxidizing agents can dope both crystalline and amorphous regions of P3HT. Moreover, the small size and near-spherical shape of the $FeCl_4^-$ anions favors a closer proximity of the dopant to the polymer backbone as compared to the conjugated and bulky rod-like F_4TCNQ molecules whose long axis tends to align parallel to the alkyl side chains. As a result, the electrical conductivity can reach up to 570 S/cm for $FeCl_3$-doped P3HT films and up to (509 ± 51) S/cm for Mo(tdf-$COF_3)_3$) leading in both cases to a very high thermoelectric power factor in the 150-160 µW m^{-1} K^{-2} range in the chain direction.[111]

Interestingly, in case of magic blue (MB), TEM shows almost no changes in lattice parameters of P3HT and the ED patterns remain almost unaltered upon doping even at high concentration of dopant.[108] Accordingly, P3HT crystals do not contain any MB molecule, their structure is identical to that of pristine undoped P3HT. Polarized UV–vis–NIR spectroscopy demonstrates that doping of P3HT crystals occurs from the interface with the surrounding amorphous zones that host MB molecules. Doping the amorphous phase of P3HT tends to generate more bipolarons and this leads to record charge conductivity up to 3000 S/cm in the chain direction. The fact that the $SbCl_6^-$ counterions are located outside the P3HT crystals that retain their pristine structure is apparently beneficial to reach very high charge conductivities. One possible reason is that the coulombic trapping of polaronic charges by counterions is thus reduced inside the crystals, suggesting that preferential location of dopant molecules inside amorphous zones is an interesting strategy to enhance transport in semi-crystalline PSCs.

In a recent study, Fenwick and coworkers investigated the impact of doping aligned P3HT films with F_4TCNQ on the thermal conductivity κ of the films.[112] Most interestingly, the thermal conductivity was observed to increase after doping and a sizable anisotropy was induced by alignment with thermal conductivities measured in the chain direction and perpendicular to it of 0.69 $W/m{\cdot}K$ and 0.14 $W/m{\cdot}K$, respectively. Most importantly, the observed increase of thermal conductivity in the rubbing direction was largely counterbalanced by the increase in charge conductivity, leading to a net increase of the thermoelectric figure of merit ZT by a factor 25 with respect to non-oriented films (ZT=0.018 at room temperature), underlying the pertinence of HTR for the preparation of TE films with enhanced performances.

II.b. Structural changes in sequentially doped PBTTT.

C_{12}-PBTTT is very effectively aligned using HTR as demonstrated by Biniek et al.[59] Aligned C_{12}-PBTTT were accordingly subjected to doping with different dopants ($FeCl_3$, F_4TCNQ, F_6TCNNQ) and the structural changes were followed mostly by TEM. Contrary to P3HT, C_{12}-PBTTT films rubbed at 125°C show a quenched liquid crystal structure without periodic alternation of amorphous and crystalline zones as seen for P3HT. This is because the backbone of C_{12}-PBTTT is more rigid than P3HT. Investigating the changes of C_{12}-PBTTT structure upon doping revealed similar trends as for P3HT. F_4TCNQ and F_6TCNNQ dopants intercalate in the crystalline domains of C_{12}-PBTTT, as demonstrated by polarized UV-Vis-NIR spectroscopy and low dose electron diffraction. With the help of polarized UV-Vis-NIR spectra, Vijayakumar et al. established the correlations between the orientation of the dopant anions and the polythiophene backbones by determining the order parameters defining the in-plane orientation of the polythiophene backbone and the molecular long axis of the dopant molecules.[102] For both dopants, the molecular long axis lies essentially in a plane that is perpendicular to the oriented PBTTT backbones. The order parameter defining in-plane orientation of dopants was found to be significantly lower for F_4TCNQ^- anions than for F_6TCNNQ^- anions. This result indicates that the F_4TCNQ dopants are distributed more randomly in the side chain layers of C_{12}-PBTTT than F_6TCNNQ.

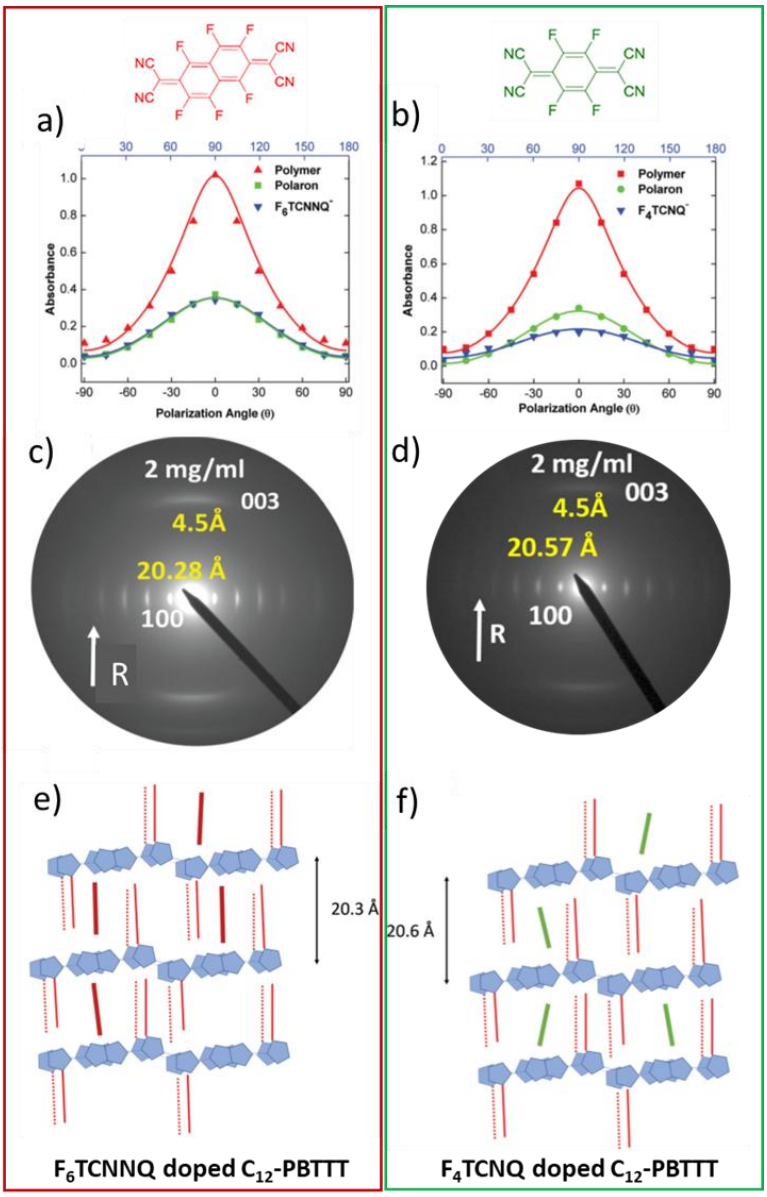

Figure 16. *a) Angular distribution of absorption bands of pristine C_{12}-PBTTT before doping, the F_6TCNNQ anion (l = 873 nm) and the P1 band (l = 2500 nm). (b) Angular distribution of the absorption bands of oriented pristine C_{12}-PBTTT before doping, the F_6TCNNQ anion (l = 1158 nm) and the polaronic P1 band (l = 2500 nm). Evolution of the electron diffraction patterns of c) F_6TCNNQ and d) F_4TCNQ doped C_{12}-PBTTT respectively at same dopant concentration using ICD method. Schematic illustration of the dopant intercalation of e) F_6TCNNQ and f) F_4TCNQ in the layers of alkyl side chains of C_{12}-PBTTT films doped by ICD. Reproduced from reference 102 with permission from the Royal Society of Chemistry.*

As for P3HT, $FeCl_3$ was used to reach higher doping levels than with F_4TCNQ and F_6TCNNQ (see Figure 16). When doped with $FeCl_3$, aligned films of C_{12}-PBTTTshow very high thermoelectric power factors of up to 3000 μW m^{-1} K^{-2} and very high electrical conductivities (1-2·10^5 S/cm) in the chain direction.[91] However, such exceptional TE properties degrade rapidly over a few hours due to the dedoping of the films. When analyzed right after doping, TEM diffraction and polarized UV-Vis-NIR spectroscopy demonstrate that $FeCl_3$ dopes both amorphous and crystalline regions of the polymer (see Figure 14). The unit cell of C_{12}-PBTTTexpands along the alkyl side chain direction (d_{100}) from 19.7 Å (pristine) to 23.6 Å (10 mM $FeCl_3$) and the π-stacking periodicity (d_{020}) is reduced, indicating that $FeCl_3$ molecules intercalate inside the layers of alkyl side chains of the crystalline phase (see Figure 17). Combination of Energy-dispersive X-ray spectroscopy and electron diffraction demonstrated that 2 $FeCl_2$ (42 $Å^3$) and 2 $FeCl_4^-$ (69 $Å^3$) can be hosted inside the unit cell of C_{12}-PBTTT as depicted in Figure 17.d. Structural investigations demonstrated thus that $FeCl_3$-doping of C_{12}-PBTTT leads to the formation of structures similar to the bimolecular crystals formed by PCBM and PBTTT.[113,114]

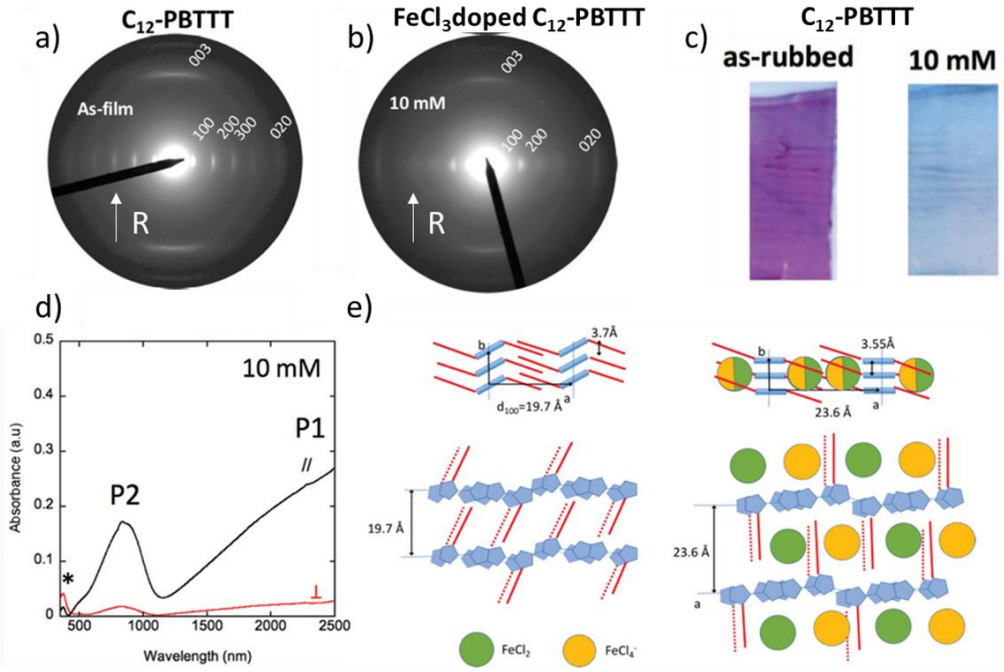

Figure 17: *Evolution of the structure of C_{12}-PBTTT obtained from low dose TEM diffraction before a) and after b) doping with 10 mM $FeCl_3$. c) Illustration of the color change in rubbed C_{12}-PBTTT films (left) upon doping with 10×10^{-3}m $FeCl_3$/nitromethane solutions. d) Polarized UV-vis-NIR spectrum in oriented C_{12}-PBTTTthin films doped with $FeCl_3$/nitromethane. e) Schematic illustration of the undoped C_{12}-PBTTT polymer and $FeCl_3$-doped C_{12}-PBTTT showing the formation of a "bimolecular crystal". Reproduced and adapted from reference 91.*

With the aim to improve TE properties in doped PBTTT, a new polymer (PBTTT-O^8) with single ether side chains (C_7-O-C_4) was designed by Durand et al.[70] The idea was to achieve similar TE properties to $FeCl_3$-doped C_{12}-PBTTT but with enhanced stability, replacing $FeCl_3$ by F_6TCNNQ. Indeed in the case of $FeCl_3$-doped C_{12}-PBTTT, the record power factor was found to be lost within a few hours under inert atmosphere, indicating some de-doping mechanism at play in the films. Very interestingly, when PBTTT-^{8}O is doped with F_6TCNNQ,

thermoelectric power factor up to 2900 µW m^{-1} K^{-2} in the chain direction were reported along with enhanced stability over $FeCl_3$-doped films.

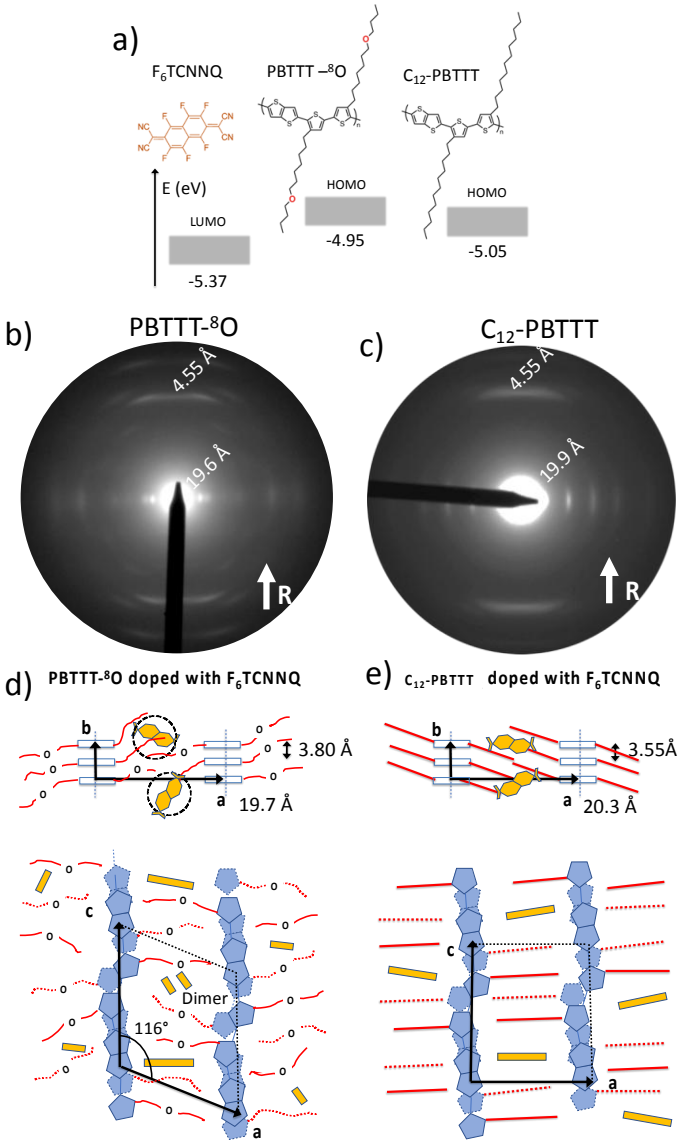

Figure 18. a) Chemical structure of F_6TCNNQ, C_{12}-PBTTTand PBTTT-^{8}O. b) and c) Electron diffraction patterns of non-doped rubbed thin films of C_{12}-PBTTTand PBTTT-^{8}O. d) and e) *Schematic representation of the dopant distributions in the layers of side chains of PBTTT-^{8}O (d) and C_{12}-PBTTT(e). Reproduced from reference 65 with permission from the Royal Society of Chemistry and from reference 70.*

The change of the side chain from C_{12} to C_7-O-C_4 in PBTTT-^{8}O does result in remarkable changes in both structure and TE properties of the PBTTT films. First, the polymer can be rubbed up to very high temperature (240°C) and optimal alignment with OP=0.86 is observed for T_R=170°C. Second, PBTTT-^{8}O shows some polymorphism in rubbed films (see Figure 18). A polymorph (form II) with reduced lamellar periodicity (d_{100} in the range 14.6-15.0 Å) is found to coexist with a classical structure (form I, d_{100} =20.6 Å) in the films rubbed at $T_R \leq 170$°C. This peculiar polymorph (form I) may involve a different tilt of the side chains to the backbone as compared to form II. The different thermomechanical properties of PBTTT-^{8}O and the very high alignment obtained in the films help reach exceptional TE properties that depend strongly on the rubbing temperature. Moreover, the chemical nature of the side chains was found to impact the dopant introduction in the polymer. With the help of polarized UV-Vis-NIR spectroscopy, Electron Spin Resonance and electron diffraction, Durand et al uncovered the mechanism of dopant insertion in the polymer crystals. In oriented PBTTT-C_{12}, $F_6TCNNQ^{\bullet-}$ dopants are inserted in the layers of interdigitated side chains with their long axis oriented perpendicular to the polymer chain direction. For this reason, the radical anion bands of $F_6TCNNQ^{\bullet-}$ are polarized in the direction orthogonal to the polymer chains. In addition, specific signatures of cofacial dimers of $F_6TCNNQ^{\bullet-}$ are found, indicating clustering of the dopants in the side chain layers of C_7-O-C_4. The order parameter has been calculated from the dichroic ratio for both the polaronic band (P1 at 2500 nm) and the dopant anion band (0-0 component at 1157 nm) which suggests that $F_6TCNNQ^{\bullet-}$ is highly ordered in the C_{12}-PBTTT lattice ($OP_{polaron}$=0.73 versus $OP_{F6TCNNQ\bullet-}$=0.70). On the contrary, in PBTTT-O^8, $F_6TCNNQ^{\bullet-}$ dopants are randomly oriented in the layers of n-C_7OC_4 side-chains (see illustration in Figure 18).[70]

Second, electron diffraction indicates that the introduction of F_6TCNNQ in the crystals of PBTTT-^{8}O results in a peculiar variation of the lattice parameters as compared to PBTTT-C_{12}. At low doping concentration, the lattice of PBTTT-^{8}O behaves similarly to that of PBTTT-C_{12}: it expands in the side chain direction and contracts in the π-stacking direction. However, as the doping level increases (≥0.5 g/l), the reverse situation is observed and the lattice parameters of the doped PBTTT-^{8}O tend to return to the pristine undoped PBTTT-^{8}O. This behavior has been attributed to the formation of dimers of the dopant anion F_6TCNNQ^-.

In a systematic study, Zeng et al. investigated the impact of the rubbing temperature and the resulting alignment on the TE properties of PBTTT-^{8}O films doped with F_6TCNNQ. The level of alignment of rubbed PBTTT-^{8}O varies with different rubbing temperature (T_R) resulting in different contact planes and orientations of the polymer.[65] Clearly, there is an optimum in in-plane orientation and crystalline order that translates into high charge conductivities in the 2-5 10^4 S/cm range and power factors > 2 mW/mK^2. Incidentally, the best TE performances of rubbed PBTTT-^{8}O were obtained for thin films rubbed at 170°C that are made of coexisting aligned edge-on and face-on crystals. Recent investigations by Wang et al. suggest that the coexistence of edge-on and face-on PSC crystals is highly beneficial to reach very high TE power factors in doped PSC films.[115]

4) Conclusion and Perspectives.

High temperature rubbing has proven to be a very effective method to fabricate aligned films of numerous p-type and n-type polymer semi-conductors. This alignment method has certain advantages over other methods such as epitaxy in terms of potential for large scale and fast roll-to-roll processing. Conversely, epitaxial crystallization opens perspectives in

terms of nano-structuring and fabrication of complex morphologies with bi-directional in-plane organization of PSC crystals that cannot be reached by the use of unidirectional shear-force alignment methods.[51] Combining HTR with controlled doping opens an interesting avenue towards the fabrication of highly oriented conducting polymer films. Such films show interesting anisotropic charge conductivity with record conductivities in the 10^4-10^5 S/cm range. So far, HTR was mainly associated to sequential doping. However, there are several alternative doping methods that should be investigated in the future in order to further improve TE properties of doped thin films. First, vapor phase doping is known to help reach better order in the doped polymer crystals thanks to a very progressive introduction of dopant molecules.[116] An additional alternative doping method is the so-called anion exchange approach originally proposed by Watanabe and coworkers.[117] Jacobs and coworkers made first attempts to use this approach on rubbed PBTTT thin films and reached charge conductivities of up to 4000 S/cm.[118] All these doping approaches open interesting perspectives to fabricate oriented conducting polymer films that can be used in numerous applications e.g. as both injecting and aligning substrates in polarized light emitting diodes. Also, from a fundamental point of view, HTR is a very effective method to crystallize PSCs in order to investigate their crystal packing and propose structural models using for instance low dose electron diffraction.[119] Aligned pristine and doped PSCs films are model systems to better understand the typical doping mechanism at play in these materials. As shown in this review, HTR can produce aligned PSC films of interest to generate anisotropic response in polarized photodetectors or dichroic photovoltaic effects in oriented solar cells. All these examples illustrate that processing of PSC films by HTR opens unique perspectives for the fabrication of new anisotropic electronic devices. Fundamental issues related to anisotropic optical and electronic properties can also more readily be analyzed from highly oriented and

structurally well-defined PSC thin films. Beyond the field of organic electronics, HTR can be applied to a range of polymers. It is for example promising to impart high crystallinity and orientation in thin films of bio-sourced polymers such as poly(lactic acid).[120,121] Besides simple polymers, more complex systems such as block copolymers with some crystallizable block(s) can also be oriented by HTR. Recent examples concern for instance poly(3-hexylthiophene)-*block*-peracetylated maltopheptaose or P3HT-*b*-P(NDI2OD-T2).[122,123] Interesting new phenomena resulting from the competing crystallization processes of the two blocks can be analyzed in details in aligned thin films. HTR proved also effective for the orientation of small molecular systems including H-bonded perylene bisimide organogelators or acceptor-donor-acceptor triad materials.[124,125] Beyond pure organic systems, HTR is also a very elegant alignment method to fabricate hybrid polymer/nanoparticle systems with the possibility to orient simultaneously anisotropic nanoparticles (nanorods) and polymer chains.[126] Taken altogether, these numerous examples support the versatility and high potential of HTR as a processing method to fabricate complex anisotropic architectures for material science purposes.

Acknowledgments.

Bernard Lotz is gratefully acknowledged for fruitful discussions and careful reading of the manuscript. Financial support from ANR grants PSLM (ANR-19-CE05-0036) and Thermopolys (ANR 2022-CE50-0020) is acknowledged. Moreover, this work was financially supported by the European Commission through Marie Sklodowska-Curie project HORATES (GA-955837).

Conflict of interest.

The authors declare no conflict of interest.

References.

(1) Ogawa, S. in *Organic Electronics*, Springer Japan, **2015**, pp 1-245.

(2) Goel, M.; Thelakkat, M. Polymer Thermoelectrics: Opportunities and Challenges. *Macromolecules* **2020**, *53* (10), 3632–3642. https://doi.org/10.1021/acs.macromol.9b02453.

(3) Kukhta, N. A.; Luscombe, C. K. Gaining Control over Conjugated Polymer Morphology to Improve the Performance of Organic Electronics. *Chem. Commun.* **2022**, *58* (50), 6982–6997. https://doi.org/10.1039/D2CC01430K.

(4) Zhang, G.; Lin, F. R.; Qi, F.; Heumüller, T.; Distler, A.; Egelhaaf, H.-J.; Li, N.; Chow, P. C. Y.; Brabec, C. J.; Jen, A. K.-Y.; Yip, H.-L. Renewed Prospects for Organic Photovoltaics. *Chem. Rev.* **2022**, *122* (18), 14180–14274. https://doi.org/10.1021/acs.chemrev.1c00955.

(5) Tatum, W. K.; Luscombe, C. K. π-Conjugated Polymer Nanowires: Advances and Perspectives toward Effective Commercial Implementation. *Polymer Journal* **2018**, *50* (8), 659–669. https://doi.org/10.1038/s41428-018-0062-6.

(6) Brinkmann, M. Structure and Morphology Control in Thin Films of Regioregular Poly(3-Hexylthiophene). *Journal of Polymer Science Part B-Polymer Physics* **2011**, *49* (17), 1218–1233. https://doi.org/10.1002/polb.22310.

(7) Rahimi, K.; Botiz, I.; Stingelin, N.; Kayunkid, N.; Sommer, M.; Koch, F. P. V.; Nguyen, H.; Coulembier, O.; Dubois, P.; Brinkmann, M.; Reiter, G. Controllable Processes for Generating

Large Single Crystals of Poly(3-Hexylthiophene). *Angewandte Chemie-International Edition* **2012**, *51* (44), 11131–11135. https://doi.org/10.1002/anie.201205653.

(8) Brinkmann, M.; Chandezon, F.; Pansu, R. B.; Julien-Rabant, C. Epitaxial Growth of Highly Oriented Fibers of Semiconducting Polymers with a Shish-Kebab-Like Superstructure. *Advanced Functional Materials* **2009**, *19* (17), 2759–2766. https://doi.org/10.1002/adfm.200900966.

(9) Crossland, E. J. W.; Tremel, K.; Fischer, F.; Rahimi, K.; Reiter, G.; Steiner, U.; Ludwigs, S. Anisotropic Charge Transport in Spherulitic Poly(3-Hexylthiophene) Films. *Advanced Materials* **2012**, *24*, 839–844. https://doi.org/10.1002/adma.201104284.

(10) Brinkmann, M.; Wittmann, J.-C. Orientation of Regioregular Poly(3-Hexylthiophene) by Directional Solidification: A Simple Method to Reveal the Semicrystalline Structure of a Conjugated Polymer. *Advanced Materials* **2006**, *18* (7), 860–863. https://doi.org/10.1002/adma.200501838.

(11) Tremel, K.; Ludwigs, S. Morphology of P3HT in Thin Films in Relation to Optical and Electrical Properties. In *P3HT Revisited – From Molecular Scale to Solar Cell Devices*; Ludwigs, S., Ed.; Springer Berlin Heidelberg: Berlin, Heidelberg, 2014; pp 39–82. https://doi.org/10.1007/12_2014_288.

(12) Lan, Y.-K.; Huang, C.-I. Charge Mobility and Transport Behavior in the Ordered and Disordered States of the Regioregular Poly(3-Hexylthiophene). *J. Phys. Chem. B* **2009**, *113* (44), 14555–14564. https://doi.org/10.1021/jp904841j.

(13) Brinkmann, M.; Hartmann, L.; Biniek, L.; Tremel, K.; Kayunkid, N. Orienting Semi-Conducting Pi-Conjugated Polymers. *Macromolecular Rapid Communications* **2014**, *35* (1), 9–26. https://doi.org/10.1002/marc.201300712

(14) Memon, W. A.; Zhang, Y.; Zhang, J.; Yan, Y.; Wang, Y.; Wei, Z. Alignment of Organic Conjugated Molecules for High-Performance Device Applications. *Macromolecular Rapid Communications* **2022**, *43* (14), 2100931. https://doi.org/10.1002/marc.202100931.

(15) Pandey, M.; Kumari, N.; Nagamatsu, S.; Pandey, S. S. Recent Advances in the Orientation of Conjugated Polymers for Organic Field-Effect Transistors. *J. Mater. Chem. C* **2019**, *7* (43), 13323–13351. https://doi.org/10.1039/C9TC04397G.

(16) Gu, X.; Shaw, L.; Gu, K.; Toney, M. F.; Bao, Z. The Meniscus-Guided Deposition of Semiconducting Polymers. *Nature Communications* **2018**, *9* (1), 534. https://doi.org/10.1038/s41467-018-02833-9.

(17) Memon, W. A.; Zhang, Y.; Zhang, J.; Yan, Y.; Wang, Y.; Wei, Z. Alignment of Organic Conjugated Molecules for High-Performance Device Applications. *Macromolecular Rapid Communications* **2022**, *43* (14), 2100931. https://doi.org/10.1002/marc.202100931.

(18) Schneider, S. A.; Gu, K. L.; Yan, H.; Abdelsamie, M.; Bao, Z.; Toney, M. F. Controlling Polymer Morphology in Blade-Coated All-Polymer Solar Cells. *Chem. Mater.* **2021**, *33* (15), 5951–5961. https://doi.org/10.1021/acs.chemmater.1c01050.

(19) Wu, D.; Kaplan, M.; Ro, H. W.; Engmann, S.; Fischer, D. A.; DeLongchamp, D. M.; Richter, L. J.; Gann, E.; Thomsen, L.; McNeill, C. R.; Zhang, X. Blade Coating Aligned, High-Performance, Semiconducting-Polymer Transistors. *Chem. Mater.* **2018**, *30* (6), 1924–1936. https://doi.org/10.1021/acs.chemmater.7b04835.

(20) Persson, N. E.; Engmann, S.; Richter, L. J.; DeLongchamp, D. M. In Situ Observation of Alignment Templating by Seed Crystals in Highly Anisotropic Polymer Transistors. *Chem. Mater.* **2019**, *31* (11), 4133–4147. https://doi.org/10.1021/acs.chemmater.9b00888.

(21) Molina-Lopez, F.; Wu, H.-C.; Wang, G.-J. N.; Yan, H.; Shaw, L.; Xu, J.; Toney, M. F.; Bao, Z. Enhancing Molecular Alignment and Charge Transport of Solution-Sheared Semiconducting Polymer Films by the Electrical-Blade Effect. *Advanced Electronic Materials* **2018**, *4* (7), 1800110. https://doi.org/10.1002/aelm.201800110.

(22) Trefz, D.; Gross, Y. M.; Dingler, C.; Tkachov, R.; Hamidi-Sakr, A.; Kiriy, A.; McNeill, C. R.; Brinkmann, M.; Ludwigs, S. Tuning Orientational Order of Highly Aggregating P(NDI2OD-T2) by Solvent Vapor Annealing and Blade Coating. *Macromolecules* **2019**, 52, 43 https://doi.org/10.1021/acs.macromol.8b02176.

(23) Meng, L.; Bian, R.; Guo, C.; Xu, B.; Liu, H.; Jiang, L. Aligning Ag Nanowires by a Facile Bioinspired Directional Liquid Transfer: Toward Anisotropic Flexible Conductive Electrodes. *Advanced Materials* **2018**, *30* (25), 1706938. https://doi.org/10.1002/adma.201706938.

(24) Guo, C.; Gao, X.; Lin, F.-J.; Wang, Q.; Meng, L.; Bian, R.; Sun, Y.; Jiang, L.; Liu, H. In Situ Characterization of the Triphase Contact Line in a Brush-Coating Process: Toward the Enhanced Efficiency of Polymer Solar Cells. *ACS Appl. Mater. Interfaces* **2018**, *10* (46), 39448–39454. https://doi.org/10.1021/acsami.8b15746.

(25) Lin, F.-J.; Chen, H.-H.; Tao, Y.-T. Molecularly Aligned Hexa-Peri-Hexabenzocoronene Films by Brush-Coating and Their Application in Thin-Film Transistors. *ACS Appl. Mater. Interfaces* **2019**, *11* (11), 10801–10809. https://doi.org/10.1021/acsami.9b00873.

(26) Lin, F.-J.; Guo, C.; Chuang, W.-T.; Wang, C.-L.; Wang, Q.; Liu, H.; Hsu, C.-S.; Jiang, L. Directional Solution Coating by the Chinese Brush: A Facile Approach to Improving Molecular Alignment for High-Performance Polymer TFTs. *Advanced Materials* **2017**, *29* (34), 1606987. https://doi.org/10.1002/adma.201606987.

(27) Xiao, X.; Pan, G.; Li, T.; Su, S.; Zhu, L.; Zhu, X.; Zhang, F. Magnetic-Field Guided Solvent Vapor Annealing for Enhanced Molecular Alignment and Carrier Mobility of a Semiconducting Diketopyrrolopyrrole-Based Polymer. *J. Mater. Chem. C* **2020**, *8* (13), 4477–4485. https://doi.org/10.1039/C9TC05803F.

(28) Pan, G.; Hu, L.; Zhang, F.; Chen, Q. Out-of-Plane Alignment of Conjugated Semiconducting Polymers by Horizontal Rotation in a High Magnetic Field. *J. Phys. Chem. Lett.* **2021**, *12* (14), 3476–3484. https://doi.org/10.1021/acs.jpclett.1c00385.

(29) Petermann, J.; Gohil, R. M. A New Method for the Preparation of High Modulus Thermoplastic Films. *Journal of Materials Science* **1979**, *14* (9), 2260–2264. https://doi.org/10.1007/BF00688435.

(30) Wang, J.; Liu, Y.; Hua, L.; Wang, T.; Dong, H.; Li, H.; Sun, X.; Ren, Z.; Yan, S. Oriented Conjugated Copolymer Films with Controlled Crystal Forms and Molecular Stacking Modes for Enhanced Charge Transport and Photoresponsivity. *ACS Appl. Polym. Mater.* **2021**, *3* (4), 2098–2108. https://doi.org/10.1021/acsapm.1c00144.

(31) Li, Y.; Xin, R.; Wang, S.; Guo, Z.; Sun, X.; Ren, Z.; Li, H.; Li, L.; Yan, S. Structure and Mechanical Property of Melt-Drawn Oriented PLA Ultrathin Films. *Macromolecules* **2021**, *54* (19), 9124–9134. https://doi.org/10.1021/acs.macromol.1c01678.

(32) O'Connor B., Kline R. J., Conrad B. R., Richter L. J., Gundlach D., Toney M. F., and DeLongchamp D. M., *Adv. Funct. Mater*., 2011, **21**, 3697–3705.

(33) Ding, Y.; Zhu, Y.; Wang, X.; Wang, Y.; Zhang, S.; Zhang, G.; Gu, X.; Qiu, L. Side Chain Engineering: Achieving Stretch-Induced Molecular Orientation and Enhanced Mobility in Polymer Semiconductors. *Chem. Mater.* **2022**, *34* (6), 2696–2707. https://doi.org/10.1021/acs.chemmater.1c04085.

(34) Wittmann, J. C.; Smith, P. Highly Oriented Thin Films of Poly(Tetrafluoroethylene) as a Substrate for Oriented Growth of Materials. *Nature* **1991**, *352* (6334), 414–417. https://doi.org/10.1038/352414a0.

(35) Nagamatsu, S.; Takashima, W.; Kaneto, K.; Yoshida, Y.; Tanigaki, N.; Yase, K.; Omote, K. Backbone Arrangement in "Friction-Transferred" Regioregular Poly(3-Alkylthiophene)s. *Macromolecules* **2003**, *36* (14), 5252–5257. https://doi.org/10.1021/ma025887t.

(36) Nagamatsu, S.; Misaki, M.; Chikamatsu, M.; Kimura, T.; Yoshida, Y.; Azumi, R.; Tanigaki, N.; Yase, K. Crystal Structure of Friction-Transferred Poly(2,5-Dioctyloxy-1,4-Phenylenevinylene). *J. Phys. Chem. B* **2007**, *111* (17), 4349–4354. https://doi.org/10.1021/jp067555m.

(37) Misaki, M.; Ueda, Y.; Nagamatsu, S.; Yoshida, Y.; Tanigaki, N.; Yase, K. Formation of Single-Crystal-like Poly(9,9-Dioctylfluorene) Thin Film by the Friction-Transfer Technique with Subsequent Thermal Treatments. *Macromolecules* **2004**, *37* (18), 6926–6931. https://doi.org/10.1021/ma049051x.

(38) Misaki, M.; Ueda, Y.; Nagamatsu, S.; Chikamatsu, M.; Yoshida, Y.; Tanigaki, N.; Yase, K. Highly Polarized Polymer Light-Emitting Diodes Utilizing Friction-Transferred Poly(9,9-Dioctylfluorene) Thin Films. *Appl. Phys. Lett.* **2005**, *87* (24), 243503. https://doi.org/10.1063/1.2142082.

(39) Hosokawa, Y.; Misaki, M.; Yamamoto, S.; Torii, M.; Ishida, K.; Ueda, Y. Molecular Orientation and Anisotropic Carrier Mobility in Poorly Soluble Polythiophene Thin Films. *Appl. Phys. Lett.* **2012**, *100* (20), 203305. https://doi.org/10.1063/1.4718424.

(40) Hooks, D. E.; Fritz, T.; Ward, M. D. Epitaxy and Molecular Organization on Solid Substrates. *Advanced Materials* **2001**, *13* (4), 227–241. https://doi.org/10.1002/1521-4095(200102)13:4<227::AID-ADMA227>3.0.CO;2-P.

(41) Wittmann, J. C.; Lotz, B. Epitaxial Crystallization of Aliphatic Polyesters on Trioxane and Various Aromatic Hydrocarbons. *Journal of Polymer Science: Polymer Physics Edition* **1981**, *19* (12), 1853–1864. https://doi.org/10.1002/pol.1981.180191205.

(42) Wittmann, J. C.; Hodge, A. M.; Lotz, B. Epitaxial Crystallization of Polymers onto Benzoic Acid: Polyethylene and Paraffins, Aliphatic Polyesters, and Polyamides. *Journal of Polymer Science: Polymer Physics Edition* **1983**, *21* (12), 2495–2509. https://doi.org/10.1002/pol.1983.180211207.

(43) Da Costa, V.; Le Moigne, J.; Oswald, L.; Pham, T. A.; Thierry, A. Thin Film Orientation by Epitaxy of Carbazolyl Polydiacetylenes: Guest−Host Interaction on a Crystal Surface. *Macromolecules* **1998**, *31* (5), 1635–1643. https://doi.org/10.1021/ma971177p.

(44) Brinkmann, M.; Hartmann, L.; Biniek, L.; Tremel, K.; Kayunkid, N. Orienting Semi-Conducting π-Conjugated Polymers. *Macromolecular Rapid Communications* **2014**, *35* (1), 9–26. https://doi.org/10.1002/marc.201300712.

(45) Brinkmann, M.; Contal, C.; Kayunkid, N.; Djuric, T.; Resel, R. Highly Oriented and Nanotextured Films of Regioregular Poly(3-Hexylthiophene) Grown by Epitaxy on the Nanostructured Surface of an Aromatic Substrate. *Macromolecules* **2010**, *43* (18), 7604–7610. https://doi.org/10.1021/ma101313m.

(46) Le Moigne, J.; Kajzar, F.; Thierry, A. Single Orientation in Poly(Diacetylene) Films for Nonlinear Optics. Molecular Epitaxy of 1,6-Bis(9-Carbazolyl)-2,4-Hexadiyne on Organic Crystals. *Macromolecules* **1991**, *24* (9), 2622–2628. https://doi.org/10.1021/ma00009a073.

(47) Jimison, L. H.; Toney, M. F.; McCulloch, I.; Heeney, M.; Salleo, A. Charge-Transport Anisotropy Due to Grain Boundaries in Directionally Crystallized Thin Films of Regioregular Poly(3-Hexylthiophene). *Advanced Materials* **2009**, *21* (16), 1568–1572. https://doi.org/10.1002/adma.200802722.

(48) Brinkmann, M.; Wittmann, J.-C. Orientation of Regioregular Poly(3-Hexylthiophene) by Directional Solidification: A Simple Method to Reveal the Semicrystalline Structure of a Conjugated Polymer. *Advanced Materials* **2006**, *18* (7), 860–863. https://doi.org/10.1002/adma.200501838.

(49) Brinkmann, M.; Rannou, P. Effect of Molecular Weight on the Structure and Morphology of Oriented Thin Films of Regioregular Poly(3-Hexylthiophene) Grown by Directional Epitaxial Solidification. *Advanced Functional Materials* **2007**, *17* (1), 101–108. https://doi.org/10.1002/adfm.200600673.

(50) Brinkmann, M.; Hartmann, L.; Kayunkid, N.; Djurado, D. Understanding the Structure and Crystallization of Regioregular Poly(3-Hexylthiophene) from the Perspective of Epitaxy. In *P3HT Revisited: From Molecular Scale to Solar Cell Devices*; Ludwigs, S., Ed.; 2014; Vol. 265, pp 83–106.

(51) Hamidi-Sakr, A.; Schiefer, D.; Covindarassou, S.; Biniek, L.; Sommer, M.; Brinkmann, M. Highly Oriented and Crystalline Films of a Phenyl-Substituted Polythiophene Prepared by Epitaxy: Structural Model and Influence of Molecular Weight. *Macromolecules* **2016**, *49* (9), 3452–3462. https://doi.org/10.1021/acs.macromol.6b00495.

(52) Brinkmann, M.; Gonthier, E.; Bogen, S.; Tremel, K.; Ludwigs, S.; Hufnagel, M.; Sommer, M. Segregated versus Mixed Interchain Stacking in Highly Oriented Films of Naphthalene Diimide Bithiophene Copolymers. *ACS Nano* **2012**, *6* (11), 10319–10326. https://doi.org/10.1021/nn304213h.

(53) Hartmann, L.; Tremel, K.; Uttiya, S.; Crossland, E.; Ludwigs, S.; Kayunkid, N.; Vergnat, C.; Brinkmann, M. 2D Versus 3D Crystalline Order in Thin Films of Regioregular Poly(3-Hexylthiophene) Oriented by Mechanical Rubbing and Epitaxy. *Advanced Functional Materials* **2011**, *21* (21), 4047–4057. https://doi.org/10.1002/adfm.201101139.

(54) Kayunkid, N.; Uttiya, S.; Brinkmann, M. Structural Model of Regioregular Poly(3-Hexylthiophene) Obtained by Electron Diffraction Analysis. *Macromolecules* **2010**, *43* (11), 4961–4967. https://doi.org/10.1021/ma100551m.

(55) Brinkmann, M.; Charoenthai, N.; Traiphol, R.; Piyakulawat, P.; Wlosnewski, J.; Asawapirom, U. Structure and Morphology in Highly Oriented Films of Poly(9,9-Bis(n-Octyl)Fluorene-2,7-Diyl) and Poly(9,9-Bis(2-Ethylhexyl)Fluorene-2,7-Diyl) Grown on Friction Transferred Poly(Tetrafluoroethylene). *Macromolecules* **2009**, *42* (21), 8298–8306. https://doi.org/10.1021/ma901623s.

(56) van Aerle, N. A. J. M.; Barmentlo, M.; Hollering, R. W. J. Effect of Rubbing on the Molecular Orientation within Polyimide Orienting Layers of Liquid-crystal Displays. *Journal of Applied Physics* **1993**, *74* (5), 3111–3120. https://doi.org/10.1063/1.354577.

(57) Toney, M. F.; Russell, T. P.; Logan, J. A.; Kikuchi, H.; Sands, J. M.; Kumar, S. K. Near-Surface Alignment of Polymers in Rubbed Films. *Nature* **1995**, *374* (6524), 709–711. https://doi.org/10.1038/374709a0.

(58) Heil, H.; Finnberg, T.; von Malm, N.; Schmechel, R.; von Seggern, H. The Influence of Mechanical Rubbing on the Field-Effect Mobility in Polyhexylthiophene. *Journal of Applied Physics* **2003**, *93* (3), 1636–1641. https://doi.org/10.1063/1.1530720.

(59) Biniek, L.; Pouget, S.; Djurado, D.; Gonthier, E.; Tremel, K.; Kayunkid, N.; Zaborova, E.; Crespo-Monteiro, N.; Boyron, O.; Leclerc, N.; Ludwigs, S.; Brinkmann, M. High-Temperature Rubbing: A Versatile Method to Align π-Conjugated Polymers without Alignment Substrate. *Macromolecules* **2014**, *47* (12), 3871–3879. https://doi.org/10.1021/ma500762x.

(60) Tremel, K.; Fischer, F. S. U.; Kayunkid, N.; Di Pietro, R.; Tkachov, R.; Kiriy, A.; Neher, D.; Ludwigs, S.; Brinkmann, M. Charge Transport Anisotropy in Highly Oriented Thin Films of the Acceptor Polymer P(NDI2OD-T2). *Advanced Energy Materials* **2014**, *4* (10), 1301659. https://doi.org/10.1002/aenm.201301659.

(61) Hamidi-Sakr, A.; Biniek, L.; Fall, S.; Brinkmann, M. Precise Control of Lamellar Thickness in Highly Oriented Regioregular Poly(3-Hexylthiophene) Thin Films Prepared by High-Temperature Rubbing: Correlations with Optical Properties and Charge Transport. *Advanced Functional Materials* **2016**, *26* (3), 408–420. https://doi.org/10.1002/adfm.201504096.

(62) Biniek, L.; Leclerc, N.; Heiser, T.; Bechara, R.; Brinkmann, M. Large Scale Alignment and Charge Transport Anisotropy of PBTTT Films Oriented by High Temperature Rubbing. *Macromolecules* **2013**, *46* (10), 4014–4023. https://doi.org/10.1021/ma400516d.

(63) Biniek, L.; Hamidi-Sakr, A.; Grodd, L.; Escoubas, S.; Dappe, Y. J.; Grigorian, S.; Schmutz, M.; Brinkmann, M. Structure and Charge Transport Anisotropy of Polythieno[3,4-b]-Thiophene-Co-Benzodithiophene (PTB7) Oriented by High-Temperature Rubbing. *Advanced Electronic Materials* **2018**, *0* (0), 1700480. https://doi.org/10.1002/aelm.201700480.

(64) Fischer, F. S. U.; Kayunkid, N.; Trefz, D.; Ludwigs, S.; Brinkmann, M. Structural Models of Poly(Cyclopentadithiophene-Alt-Benzothiadiazole) with Branched Side Chains: Impact of a Single Fluorine Atom on the Crystal Structure and Polymorphism of a Conjugated Polymer. *Macromolecules* **2015**, *48* (12), 3974–3982. https://doi.org/10.1021/acs.macromol.5b00839.

(65) Zeng, H.; Durand, P.; Guchait, S.; Herrmann, L.; Kiefer, C.; Leclerc, N.; Brinkmann, M. Optimizing Chain Alignment and Preserving the Pristine Structure of Single-Ether Based PBTTT Helps Improve Thermoelectric Properties in Sequentially Doped Thin Films. *J. Mater. Chem. C* **2022**, *10* (42), 15883–15896. https://doi.org/10.1039/D2TC03600B.

(66) Zeng, H.; Mohammed, M.; Untilova, V.; Boyron, O.; Berton, N.; Limelette, P.; Schmaltz, B.; Brinkmann, M. Fabrication of Oriented N-Type Thermoelectric Polymers by Polarity Switching in a DPP-Based Donor–Acceptor Copolymer Doped with FeCl3. *Advanced Electronic Materials* **2021**, *7* (5), 2000880. https://doi.org/10.1002/aelm.202000880.

(67) McCulloch, I.; Heeney, M.; Bailey, C.; Genevicius, K.; MacDonald, I.; Shkunov, M.; Sparrowe, D.; Tierney, S.; Wagner, R.; Zhang, W.; Chabinyc, M. L.; Kline, R. J.; McGehee, M. D.; Toney, M. F. Liquid-Crystalline Semiconducting Polymers with High Charge-Carrier Mobility. *Nature Materials* **2006**, *5* (4), 328–333. https://doi.org/10.1038/nmat1612.

(68) DeLongchamp, D. M.; Kline, R. J.; Jung, Y.; Germack, D. S.; Lin, E. K.; Moad, A. J.; Richter, L. J.; Toney, M. F.; Heeney, M.; McCulloch, I. Controlling the Orientation of Terraced Nanoscale “Ribbons” of a Poly(Thiophene) Semiconductor. *ACS Nano* **2009**, *3* (4), 780–787. https://doi.org/10.1021/nn800574f.

(69) DeLongchamp, D. M.; Kline, R. J.; Jung, Y.; Lin, E. K.; Fischer, D. A.; Gundlach, D. J.; Cotts, S. K.; Moad, A. J.; Richter, L. J.; Toney, M. F.; Heeney, M.; McCulloch, I. Molecular Basis of

Mesophase Ordering in a Thiophene-Based Copolymer. *Macromolecules* **2008**, *41* (15), 5709–5715. https://doi.org/10.1021/ma800440f.

(70) Durand, P.; Zeng, H.; Biskup, T.; Vijayakumar, V.; Untilova, V.; Kiefer, C.; Heinrich, B.; Herrmann, L.; Brinkmann, M.; Leclerc, N. Single Ether-Based Side Chains in Conjugated Polymers: Toward Power Factors of 2.9 MW M−1 K−2. *Advanced Energy Materials* **2022**, *12* (2), 2103049. https://doi.org/10.1002/aenm.202103049.

(71) Zhong, Y.; Biniek, L.; Leclerc, N.; Ferry, S.; Brinkmann, M. Segregated versus Disordered Stacking in Two Low Bandgap Alternated Copolymers for Photovoltaic Applications: Impact of Polymorphism on Optical Properties. *Macromolecules* **2018**, *51* (11), 4238–4249. https://doi.org/10.1021/acs.macromol.8b00378.

(72) Vohra, V.; Arrighetti, G.; Barba, L.; Higashimine, K.; Porzio, W.; Murata, H. Enhanced Vertical Concentration Gradient in Rubbed P3HT:PCBM Graded Bilayer Solar Cells. *J. Phys. Chem. Lett.* **2012**, *3* (13), 1820–1823. https://doi.org/10.1021/jz300710a.

(73) Zhu, R.; Kumar, A.; Yang, Y. Polarizing Organic Photovoltaics. *Advanced Materials* **2011**, *23* (36), 4193–4198. https://doi.org/10.1002/adma.201101514.

(74) Schrickx, H. M.; Sen, P.; Booth, R. E.; Altaqui, A.; Burleson, J.; Rech, J. J.; Lee, J.-W.; Biliroglu, M.; Gundogdu, K.; Kim, B. J.; You, W.; Kudenov, M. W.; O'Connor, B. T. Ultra-High Alignment of Polymer Semiconductor Blends Enabling Photodetectors with Exceptional

Polarization Sensitivity. *Advanced Functional Materials* **2022**, *32* (2), 2105820. https://doi.org/10.1002/adfm.202105820.

(75) Fall, S.; Wang, J.; Regrettier, T.; Brouckaert, N.; Ibraikulov, O. A.; Leclerc, N.; Lin, Y.; Elhaj, M. I.; Komitov, L.; Lévêque, P.; Zhong, Y.; Brinkmann, M.; Kaczmarek, M.; Heiser, T. Self-Powered Dynamic Glazing Based on Nematic Liquid Crystals and Organic Photovoltaic Layers for Smart Window Applications. *ACS Appl. Mater. Interfaces* **2023**, *15* (3), 4267–4274. https://doi.org/10.1021/acsami.2c21727.

(76) Yang, D. K.; Wu, S. T. *Fundamentals of Liquid Crystal Devices*; Wiley, 2015; p 127.

(77) Shirakawa, H.; Louis, E. J.; MacDiarmid, A. G.; Chiang, C. K.; Heeger, A. J. Synthesis of Electrically Conducting Organic Polymers: Halogen Derivatives of Polyacetylene, (CH) x. *J. Chem. Soc. Chem. Commun.* **1977**, No. 16, 578. https://doi.org/10.1039/c39770000578.

(78) Pron, A.; Rannou, P. Processible Conjugated Polymers: From Organic Semiconductors to Organic Metals and Superconductors. *Prog. Polym. Sci.* **2002**, *27* (1), 135–190. https://doi.org/10.1016/S0079-6700(01)00043-0.

(79) Hatchett, D. W.; Josowicz, M.; Janata, J. Acid Doping of Polyaniline: Spectroscopic and Electrochemical Studies. *J. Phys. Chem. B* **1999**, *103* (50), 10992–10998. https://doi.org/10.1021/jp991110z.

(80) Fahlman, M.; Fabiano, S.; Gueskine, V.; Simon, D.; Berggren, M.; Crispin, X. Interfaces in Organic Electronics. *Nat. Rev. Mater.* **2019**, *4* (10), 627–650. https://doi.org/10.1038/s41578-019-0127-y.

(81) Lüssem, B.; Keum, C.-M.; Kasemann, D.; Naab, B.; Bao, Z.; Leo, K. Doped Organic Transistors. *Chem. Rev.* **2016**, *116* (22), 13714–13751. https://doi.org/10.1021/acs.chemrev.6b00329.

(82) Russ, B.; Glaudell, A.; Urban, J. J.; Chabinyc, M. L.; Segalman, R. A. Organic Thermoelectric Materials for Energy Harvesting and Temperature Control. *Nat. Rev. Mater.* **2016**, *1* (10), 16050. https://doi.org/10.1038/natrevmats.2016.50.

(83) Bubnova, O.; Khan, Z. U.; Malti, A.; Braun, S.; Fahlman, M.; Berggren, M.; Crispin, X. Optimization of the Thermoelectric Figure of Merit in the Conducting Polymer Poly(3,4-Ethylenedioxythiophene). *Nat. Mater.* **2011**, *10* (6), 429–433. https://doi.org/10.1038/nmat3012.

(84) Kroon, R.; Mengistie, D. A.; Kiefer, D.; Hynynen, J.; Ryan, J. D.; Yu, L.; Müller, C. Thermoelectric Plastics: From Design to Synthesis, Processing and Structure–Property Relationships. *Chem. Soc. Rev.* **2016**, *45* (22), 6147–6164. https://doi.org/10.1039/C6CS00149A.

(85) Salleo, A.; Kline, R. J.; DeLongchamp, D. M.; Chabinyc, M. L. Microstructural Characterization and Charge Transport in Thin Films of Conjugated Polymers. *Adv. Mater.* **2010**, *22* (34), 3812–3838. https://doi.org/10.1002/adma.200903712.

(86) Sirringhaus, H.; Brown, P. J.; Friend, R. H.; Nielsen, M. M.; Bechgaard, K.; Langeveld-Voss, B. M. W.; Spiering, A. J. H.; Janssen, R. A. J.; Meijer, E. W.; Herwig, P.; de Leeuw, D. M. Two-Dimensional Charge Transport in Self-Organized, High-Mobility Conjugated Polymers. *Nature* **1999**, *401* (6754), 685–688. https://doi.org/10.1038/44359.

(87) Duong, D. T.; Wang, C.; Antono, E.; Toney, M. F.; Salleo, A. The Chemical and Structural Origin of Efficient P-Type Doping in P3HT. *Org. Electron.* **2013**, *14* (5), 1330–1336. https://doi.org/10.1016/j.orgel.2013.02.028.

(88) Li, W.; Yang, L.; Tumbleston, J. R.; Yan, L.; Ade, H.; You, W. Controlling Molecular Weight of a High Efficiency Donor-Acceptor Conjugated Polymer and Understanding Its Significant Impact on Photovoltaic Properties. *Adv. Mater.* **2014**, *26* (26), 4456–4462. https://doi.org/10.1002/adma.201305251.

(89) Park, Y. W.; Park, C.; Lee, Y. S.; Yoon, C. O.; Shirakawa, H.; Suezaki, Y.; Akagi, K. Electrical Conductivity of Highly-Oriented-Polyacetylene. *Solid State Commun.* **1988**, *65* (2), 147–150. https://doi.org/10.1016/0038-1098(88)90675-8.

(90) Kivelson, S.; Heeger, A. J. Intrinsic Conductivity of Conducting Polymers. *Synth. Met.* **1988**, *22* (4), 371–384. https://doi.org/10.1016/0379-6779(88)90108-7.

(91) Vijayakumar, V.; Zhong, Y.; Untilova, V.; Bahri, M.; Herrmann, L.; Biniek, L.; Leclerc, N.; Brinkmann, M. Bringing Conducting Polymers to High Order: Toward Conductivities beyond 10^{5} S Cm^{-1} and Thermoelectric Power Factors of 2 MW m^{-1} K^{-2}. *Adv. Energy Mater.* **2019**, *9* (24), 1900266. https://doi.org/10.1002/aenm.201900266.

(92) Hamidi-Sakr, A.; Biniek, L.; Bantignies, J.-L.; Maurin, D.; Herrmann, L.; Leclerc, N.; Lévêque, P.; Vijayakumar, V.; Zimmermann, N.; Brinkmann, M. A Versatile Method to Fabricate Highly In-Plane Aligned Conducting Polymer Films with Anisotropic Charge Transport and Thermoelectric Properties: The Key Role of Alkyl Side Chain Layers on the Doping Mechanism. *Adv. Funct. Mater.* **2017**, *27* (25), 1700173. https://doi.org/10.1002/adfm.201700173.

(93) Schultheiss, A.; Revaux, A.; Carella, A.; Brinkmann, M.; Zeng, H.; Demadrille, R.; Simonato, J.-P. Electrical and Mechanical Properties of Intrinsically Flexible and Stretchable PEDOT Polymers for Thermotherapy. ACS Appl. Polym. Mater. 2021, 3 (11), 5942–5949. https://doi.org/10.1021/acsapm.1c01203.

(94) Jacobs, I. E.; Aasen, E. W.; Oliveira, J. L.; Fonseca, T. N.; Roehling, J. D.; Li, J.; Zhang, G.; Augustine, M. P.; Mascal, M.; Moulé, A. J. Comparison of Solution-Mixed and Sequentially Processed P3HT:F4TCNQ Films: Effect of Doping-Induced Aggregation on Film Morphology. *J Mater Chem C* **2016**, *4* (16), 3454–3466. https://doi.org/10.1039/C5TC04207K.

(95) Hynynen, J.; Kiefer, D.; Yu, L.; Kroon, R.; Munir, R.; Amassian, A.; Kemerink, M.; Müller, C. Enhanced Electrical Conductivity of Molecularly P-Doped Poly(3-Hexylthiophene) through Understanding the Correlation with Solid-State Order. *Macromolecules* **2017**, *50* (20), 8140–8148. https://doi.org/10.1021/acs.macromol.7b00968.

(96) Cochran, J. E.; Junk, M. J. N.; Glaudell, A. M.; Miller, P. L.; Cowart, J. S.; Toney, M. F.; Hawker, C. J.; Chmelka, B. F.; Chabinyc, M. L. Molecular Interactions and Ordering in Electrically Doped Polymers: Blends of PBTTT and F $_4$ TCNQ. *Macromolecules* **2014**, *47* (19), 6836–6846. https://doi.org/10.1021/ma501547h.

(97) Patel, S. N.; Glaudell, A. M.; Peterson, K. A.; Thomas, E. M.; O'Hara, K. A.; Lim, E.; Chabinyc, M. L. Morphology Controls the Thermoelectric Power Factor of a Doped Semiconducting Polymer. *Sci. Adv.* **2017**, *3* (6), e1700434. https://doi.org/10.1126/sciadv.1700434.

(98) Aziz, E. F.; Vollmer, A.; Eisebitt, S.; Eberhardt, W.; Pingel, P.; Neher, D.; Koch, N. Localized Charge Transfer in a Molecularly Doped Conducting Polymer. *Adv. Mater.* **2007**, *19* (20), 3257–3260. https://doi.org/10.1002/adma.200700926.

(99) Duong, D. T.; Wang, C.; Antono, E.; Toney, M. F.; Salleo, A. The Chemical and Structural Origin of Efficient P-Type Doping in P3HT. *Org. Electron.* **2013**, *14* (5), 1330–1336. https://doi.org/10.1016/j.orgel.2013.02.028.

(100) Scholes, D. T.; Hawks, S. A.; Yee, P. Y.; Wu, H.; Lindemuth, J. R.; Tolbert, S. H.; Schwartz, B. J. Overcoming Film Quality Issues for Conjugated Polymers Doped with F_4TCNQ by Solution Sequential Processing: Hall Effect, Structural, and Optical Measurements. *J. Phys. Chem. Lett.* **2015**, *6* (23), 4786–4793. https://doi.org/10.1021/acs.jpclett.5b02332.

(101) Duong, D. T.; Phan, H.; Hanifi, D.; Jo, P. S.; Nguyen, T.-Q.; Salleo, A. Direct Observation of Doping Sites in Temperature-Controlled, p-Doped P3HT Thin Films by Conducting Atomic Force Microscopy. *Adv. Mater.* **2014**, *26* (35), 6069–6073. https://doi.org/10.1002/adma.201402015.

(102) Vijayakumar, V.; Durand, P.; Zeng, H.; Untilova, V.; Herrmann, L.; Algayer, P.; Leclerc, N.; Brinkmann, M. Influence of Dopant Size and Doping Method on the Structure and Thermoelectric Properties of PBTTT Films Doped with F_6TCNNQ and F_4TCNQ. *J. Mater. Chem. C* **2020**, *8* (46), 16470–16482. https://doi.org/10.1039/D0TC02828B.

(103) Untilova, V.; Biskup, T.; Biniek, L.; Vijayakumar, V.; Brinkmann, M. Control of Chain Alignment and Crystallization Helps Enhance Charge Conductivities and Thermoelectric Power Factors in Sequentially Doped P3HT:F4TCNQ Films. *Macromolecules* **2020**, *53* (7), 2441–2453. https://doi.org/10.1021/acs.macromol.9b02389.

(104) Karpov, Y.; Erdmann, T.; Stamm, M.; Lappan, U.; Guskova, O.; Malanin, M.; Raguzin, I.; Beryozkina, T.; Bakulev, V.; Günther, F.; Gemming, S.; Seifert, G.; Hambsch, M.; Mannsfeld, S.; Voit, B.; Kiriy, A. Molecular Doping of a High Mobility Diketopyrrolopyrrole–

Dithienylthieno[3,2-b]Thiophene Donor–Acceptor Copolymer with F6TCNNQ. *Macromolecules* **2017**, *50* (3), 914–926. https://doi.org/10.1021/acs.macromol.6b02452.

(105) Enengl, C.; Enengl, S.; Pluczyk, S.; Havlicek, M.; Lapkowski, M.; Neugebauer, H.; Ehrenfreund, E. Doping-Induced Absorption Bands in P3HT: Polarons and Bipolarons. *ChemPhysChem* **2016**, *17* (23), 3836–3844. https://doi.org/10.1002/cphc.201600961.

(106) Bruchlos, K.; Trefz, D.; Hamidi-Sakr, A.; Brinkmann, M.; Heinze, J.; Ruff, A.; Ludwigs, S. Poly(3-Hexylthiophene) Revisited – Influence of Film Deposition on the Electrochemical Behaviour and Energy Levels. *Electrochimica Acta* **2018**, *269*, 299–311. https://doi.org/10.1016/j.electacta.2018.02.126.

(107) Neusser, D.; Malacrida, C.; Kern, M.; Gross, Y. M.; van Slageren, J.; Ludwigs, S. High Conductivities of Disordered P3HT Films by an Electrochemical Doping Strategy. *Chem. Mater.* **2020**, *32* (14), 6003–6013. https://doi.org/10.1021/acs.chemmater.0c01293.

(108) Zhong, Y.; Untilova, V.; Muller, D.; Guchait, S.; Kiefer, C.; Herrmann, L.; Zimmermann, N.; Brosset, M.; Heiser, T.; Brinkmann, M. Preferential Location of Dopants in the Amorphous Phase of Oriented Regioregular Poly(3-Hexylthiophene-2,5-Diyl) Films Helps Reach Charge Conductivities of 3000 S Cm−1. *Advanced Functional Materials* **2022**, *32,* 2202075. https://doi.org/10.1002/adfm.202202075.

(109) Untilova, V.; Zeng, H.; Durand, P.; Herrmann, L.; Leclerc, N.; Brinkmann, M. Intercalation and Ordering of F6TCNNQ and F4TCNQ Dopants in Regioregular Poly(3-

Hexylthiophene) Crystals: Impact on Anisotropic Thermoelectric Properties of Oriented Thin Films. *Macromolecules* **2021**, *54* (13), 6073–6084. https://doi.org/10.1021/acs.macromol.1c00554.

(110) Tashiro, K.; Kobayashi, M.; Kawai, T.; Yoshino, K. Crystal Structural Change in Poly(3-Alkyl Thiophene)s Induced by Iodine Doping as Studied by an Organized Combination of X-Ray Diffraction, Infrared/Raman Spectroscopy and Computer Simulation Techniques. *Polymer* **1997**, *38* (12), 2867–2879. https://doi.org/10.1016/S0032-3861(96)00876-2.

(111) Untilova, V.; Hynynen, J.; Hofmann, A. I.; Scheunemann, D.; Zhang, Y.; Barlow, S.; Kemerink, M.; Marder, S. R.; Biniek, L.; Müller, C.; Brinkmann, M. High Thermoelectric Power Factor of Poly(3-Hexylthiophene) through In-Plane Alignment and Doping with a Molybdenum Dithiolene Complex. *Macromolecules* **2020**, *53* (15), 6314–6321. https://doi.org/10.1021/acs.macromol.0c01223.

(112) Degousée, T.; Untilova, V.; Vijayakumar, V.; Xu, X.; Sun, Y.; Palma, M.; Brinkmann, M.; Biniek, L.; Fenwick, O. High Thermal Conductivity States and Enhanced Figure of Merit in Aligned Polymer Thermoelectric Materials. *J. Mater. Chem. A* **2021**, *9* (29), 16065–16075. https://doi.org/10.1039/D1TA03377H.

(113) Cates, N.; Cho, E.; Gysel, R.; Risko, C.; Coropceanu, V.; Miller, C. E.; Sweetnam, S.; Sellinger, A.; Heeney, M.; McCulloch, I.; Brédas, J.-L.; Toney, M. F.; McGehee, M. D. Factors Governing Intercalation of Fullerenes and Other Small Molecules Between the Side Chains of

Semiconducting Polymers Used in Solar Cells. *Advanced Energy Materials* **2012**, *2* (10), 1208–1217. https://doi.org/10.1002/aenm.201200392.

(114) Cates, N.; Cho, E.; Junk, M. J. N.; Gysel, R.; Risko, C.; Kim, D.; Sweetnam, S.; Miller, C. E.; Richter, L. J.; Kline, R. J.; Heeney, M.; McCulloch, I.; Amassian, A.; Acevedo-Feliz, D.; Knox, C.; Hansen, M. R.; Dudenko, D.; Chmelka, B. F.; Toney, M. F.; Brédas, J.-L.; McGehee, M. D. Use of X-Ray Diffraction, Molecular Simulations, and Spectroscopy to Determine the Molecular Packing in a Polymer-Fullerene Bimolecular Crystal. *Advanced Materials* **2012**, *24* (45), 6071–6079. https://doi.org/10.1002/adma.201202293.

(115) Wang, D.; Ding, J.; Dai, X.; Xiang, L.; Ye, D.; He, Z.; Zhang, F.; Jung, S.-H.; Lee, J.-K.; Di, C.; Zhu, D. Triggering ZT to 0.40 by Engineering Orientation in One Polymeric Semiconductor. *Advanced Materials* **2023**, *35* (2), 2208215. https://doi.org/10.1002/adma.202208215.

(116) Patel, S. N.; Glaudell, A. M.; Kiefer, D.; Chabinyc, M. L. Increasing the Thermoelectric Power Factor of a Semiconducting Polymer by Doping from the Vapor Phase. *ACS Macro Letters* **2016**, *5* (3), 268–272. https://doi.org/10.1021/acsmacrolett.5b00887.

(117) Yamashita, Y.; Tsurumi, J.; Ohno, M.; Fujimoto, R.; Kumagai, S.; Kurosawa, T.; Okamoto, T.; Takeya, J.; Watanabe, S. Efficient Molecular Doping of Polymeric Semiconductors Driven by Anion Exchange. *Nature* **2019**, *572* (7771), 634–638. https://doi.org/10.1038/s41586-019-1504-9.

(118) Huang, Y.; Lukito Tjhe, D. H.; Jacobs, I. E.; Jiao, X.; He, Q.; Statz, M.; Ren, X.; Huang, X.; McCulloch, I.; Heeney, M.; McNeill, C.; Sirringhaus, H. Design of Experiment Optimization of

Aligned Polymer Thermoelectrics Doped by Ion-Exchange. *Appl. Phys. Lett.* **2021**, *119* (11), 111903. https://doi.org/10.1063/5.0055886.

(119) Brinkmann, M. Insights into the Structural Complexity of Semi-Crystalline Polymer Semiconductors: Electron Diffraction Contributions. *Mater. Chem. Front.* **2020**, *4* (7), 1916–1929. https://doi.org/10.1039/D0QM00230E.

(120) Brosset, M.; Herrmann, L.; Kiefer, C.; Falher, T.; Brinkmann, M. Controlling Orientation, Polymorphism, and Crystallinity in Thin Films of Poly(Lactic-Acid) Homopolymer and Stereocomplex Aligned by High Temperature Rubbing. *Journal of Applied Polymer Science* **2023**, *140* (8), e53532. https://doi.org/10.1002/app.53532.

(121) Brosset, M.; Herrmann, L.; Falher, T.; Brinkmann, M. Preparation of Oriented Poly(Lactic Acid) Thin Films by a Combination of High Temperature Rubbing and Thermal Annealing: Impact of Annealing Parameters on Structure, Polymorphism and Morphology. *Journal of Polymer Science* **2023**, *61* (9), 829–841. https://doi.org/10.1002/pol.20220740.

(122) Sakai-Otsuka, Y.; Nishiyama, Y.; Putaux, J.-L.; Brinkmann, M.; Satoh, T.; Chen, W.-C.; Borsali, R. Competing Molecular Packing of Blocks in a Lamella-Forming Carbohydrate-Block-Poly(3-Hexylthiophene) Copolymer. *Macromolecules* **2020**, *53* (20), 9054–9064. https://doi.org/10.1021/acs.macromol.0c01801.

(123) Untilova, V.; Nübling, F.; Biniek, L.; Sommer, M.; Brinkmann, M. Impact of Competing Crystallization Processes on the Structure of All-Conjugated Donor–Acceptor Block

Copolymers P3HT-b-PNDIT2 in Highly Oriented Thin Films. *ACS Appl. Polym. Mater.* **2019**, *1* (7), 1660–1671. https://doi.org/10.1021/acsapm.9b00220.

(124) Sarbu, A.; Hermet, P.; Maurin, D.; Djurado, D.; Biniek, L.; Diebold, M.; Bantignies, J.-L.; Mesini, P.; Brinkmann, M. Supramolecular Organization of a H-Bonded Perylene Bisimide Organogelator Determined by Transmission Electron Microscopy, Grazing Incidence X-Ray Diffraction and Polarized Infra-Red Spectroscopy. *Physical Chemistry Chemical Physics* **2017**, *19* (48), 32514–32525. https://doi.org/10.1039/c7cp06761e.

(125) Rolland, D.; Brauer, J. C.; Hartmann, L.; Biniek, L.; Brinkmann, M.; Banerji, N.; Frauenrath, H. Charge Separation in an Acceptor-Donor-Acceptor Triad Material with a Lamellar Structure. *Journal of Materials Chemistry C* **2017**, *5* (6), 1383–1393. https://doi.org/10.1039/c6tc03786k.

(126) Hartmann, L.; Djurado, D.; Florea, I.; Legrand, J.-F.; Fiore, A.; Reiss, P.; Doyle, S.; Vorobiev, A.; Pouget, S.; Chandezon, F.; Ersen, O.; Brinkmann, M. Large-Scale Simultaneous Orientation of CdSe Nanorods and Regioregular Poly(3-Hexylthiophene) by Mechanical Rubbing. *Macromolecules* **2013**, *46* (15), 6177–6186. https://doi.org/10.1021/ma400880x.